

# On completeness of algebraic ZX-calculus over arbitrary commutative rings and semirings

Quanlong Wang

Department of Computer Science, University of Oxford  
Cambridge Quantum Computing Ltd.

## Abstract

ZX-calculus is a strict mathematical formalism for graphical quantum computing which is based on the field of complex numbers. In this paper, we extend its power by generalising ZX-calculus to such an extent that it both in an arbitrary commutative ring and an arbitrary commutative semiring. We follow the framework of [14] to prove that the proposed ZX-calculus over an arbitrary commutative ring is complete for matrices over the same ring, via a normal form inspired from matrix elementary operations such as row addition and row multiplication. This work paves the way for doing elementary number theory in string diagrams. The proof of completeness for ZX-calculus over arbitrary commutative semirings is quite similar, whose details will be provided in a forthcoming version.

## 1 Introduction

The ZX-calculus was introduced by Coecke and Duncan [3] as a graphical language for quantum computing, especially for quantum circuits [6]. The core part of ZX-calculus is a pair of spiders (based on the quantum Z observable and X observable) with strong complementarity [4]. As a graphical language with string diagrams, the ZX-calculus is quite intuitive. Moreover, it is also mathematically strict: the ZX-calculus dwells in a compact closed category as well as being a PROP [11], thus it is usually presented in terms of generators and rewriting rules.

Until now, the ZX-calculus has been focused on the particular algebraic object  $\mathbb{C}$ : rewriting of ZX-calculus diagrams corresponds to algebraic operations on matrices over the field of complex numbers. On the other hand, the ZW-calculus, another graphical language for quantum computing [7], has been generalised to arbitrary commutative rings by Amar Hadzihasanovic [8] [9]. This generalisation has brought forth applications in the proof of completeness of ZX-calculus for some fragments of quantum computing [10] [12]. Therefore, it is natural to ask whether ZX-calculus can also be generalised to arbitrary commutative rings, or even more broadly, to arbitrary commutative semirings.

In the case of the ZX-calculus over an arbitrary commutative ring  $\mathcal{R}$ , we can not have the same Hadamard node such as used in [3], due to lack of element like  $\frac{1}{\sqrt{2}}$  in a

general commutative ring. Similarly, for arbitrary commutative rings, we can not have the exactly same red spiders as usual. In the case of the ZX-calculus over an arbitrary commutative semiring  $\mathcal{S}$ , we even can not have a Hadamard node, since there is no negative element now. For the same reason, we do not have an inverse of the triangle node. The red spider for the semiring case is the same as that of the ring case.

In this paper, based on the framework as given in [13], we describe generalisations of ZX-calculus over arbitrary commutative rings and arbitrary commutative semirings respectively, by giving the corresponding generators and rewriting rules. Furthermore, following [14], we give the proof of completeness for ZX-calculus over arbitrary commutative rings. The key idea here is to use a normal form presented in [14] based on elementary matrix operations. For the sake of simplicity, we only give details of proofs which don't hold for general commutative rings. As one can imagine, this work paves the way for doing elementary number theory in string diagrams. The proof of completeness for ZX-calculus over arbitrary commutative semirings is quite similar, we leave the details for a forthcoming version.

## 2 ZX-calculus over commutative rings

The ZX-calculus is based on a compact closed PROP [11], which is a strict symmetric monoidal category whose objects are generated by one object, with a compact structure [5] as well. Each PROP can be described as a presentation in terms of generators and relations [2].

Since now we are working over an arbitrary commutative ring  $\mathcal{R}$ , we won't expect to have the same Hadamard node such as used in [3]. Instead, we work in the framework as presented in [13], and use a Hadamard node whose corresponding matrix is scalar-free (each element is either 1 or  $-1$  in the Hadamard matrix). For the same reason, we use a scalar-free red spider as a generator, with all the coefficients of the terms being 1 in the summation which represents the corresponding map of the red spider. Already having this, we can give the generators of ZX-calculus over  $\mathcal{R}$  in the following table. Note that through out this abstract all the diagrams should be read from top to bottom.

$R_{Z,a}^{(n,m)} : n \rightarrow m$	$R_X^{(n,m)} : n \rightarrow m$
$H : 1 \rightarrow 1$	$\sigma : 2 \rightarrow 2$
$\mathbb{I} : 1 \rightarrow 1$	$P : 1 \rightarrow 1$
$C_a : 0 \rightarrow 2$	$C_u : 2 \rightarrow 0$
$T : 1 \rightarrow 1$	$T^{-1} : 1 \rightarrow 1$

Table 1: Generators of ZX-calculus, where  $m, n \in \mathbb{N}$ ,  $a \in \mathcal{R}$ .

There is a standard interpretation  $\llbracket \cdot \rrbracket$  for the ZX diagrams over  $\mathcal{R}$ :

$$\llbracket \begin{array}{c} n \\ \backslash \diagup \diagdown / \\ m \end{array} \rrbracket = |0\rangle^{\otimes m} \langle 0|^{\otimes n} + a |1\rangle^{\otimes m} \langle 1|^{\otimes n}, \quad \llbracket \begin{array}{c} n \\ \diagup \diagdown / \backslash \\ m \end{array} \rrbracket = \sum_{\substack{i_1, \dots, i_m, j_1, \dots, j_n \in \{0,1\} \\ i_1 + \dots + i_m \equiv j_1 + \dots + j_n \pmod{2}}} |i_1, \dots, i_m\rangle \langle j_1, \dots, j_n|,$$

$$\llbracket \begin{array}{|c|} \hline \square \\ \hline \end{array} \rrbracket = \begin{pmatrix} 1 & 1 \\ 1 & -1 \end{pmatrix}, \quad \llbracket \begin{array}{|c|} \hline \Delta \\ \hline \end{array} \rrbracket = \begin{pmatrix} 1 & 1 \\ 0 & 1 \end{pmatrix}, \quad \llbracket \begin{array}{|c|} \hline \Delta^{-1} \\ \hline \end{array} \rrbracket = \begin{pmatrix} 1 & -1 \\ 0 & 1 \end{pmatrix}, \quad \llbracket \begin{array}{|c|} \hline \text{π} \\ \hline \end{array} \rrbracket = \begin{pmatrix} 0 & 1 \\ 1 & 0 \end{pmatrix}, \quad \llbracket \begin{array}{|c|} \hline \mathbb{I} \\ \hline \end{array} \rrbracket = \begin{pmatrix} 1 & 0 \\ 0 & 1 \end{pmatrix},$$

$$\llbracket \begin{array}{|c|} \hline \times \\ \hline \end{array} \rrbracket = \begin{pmatrix} 1 & 0 & 0 & 0 \\ 0 & 0 & 1 & 0 \\ 0 & 1 & 0 & 0 \\ 0 & 0 & 0 & 1 \end{pmatrix}, \quad \llbracket \begin{array}{|c|} \hline \curvearrowleft \\ \hline \end{array} \rrbracket = \begin{pmatrix} 1 \\ 0 \\ 0 \\ 1 \end{pmatrix}, \quad \llbracket \begin{array}{|c|} \hline \curvearrowright \\ \hline \end{array} \rrbracket = \begin{pmatrix} 1 & 0 & 0 & 1 \end{pmatrix}, \quad \llbracket \begin{array}{|c|} \hline \cdot \cdot \cdot \\ \hline \cdot \cdot \cdot \\ \hline \end{array} \rrbracket = 1,$$

$$\llbracket D_1 \otimes D_2 \rrbracket = \llbracket D_1 \rrbracket \otimes \llbracket D_2 \rrbracket, \quad \llbracket D_1 \circ D_2 \rrbracket = \llbracket D_1 \rrbracket \circ \llbracket D_2 \rrbracket,$$

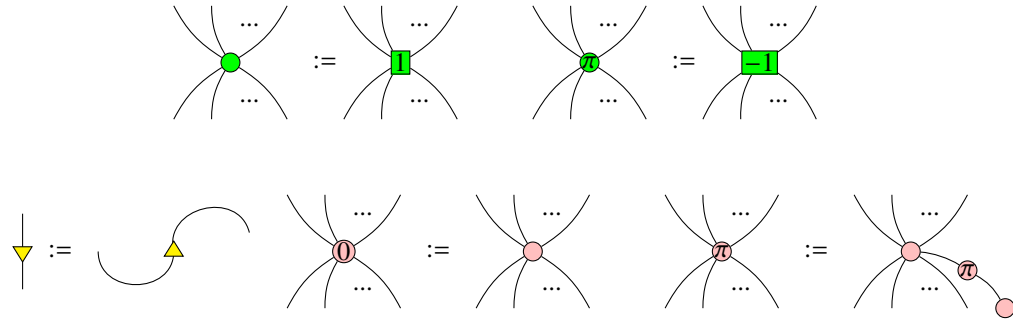
where

$$a \in \mathcal{R}, \quad |0\rangle = \begin{pmatrix} 1 \\ 0 \end{pmatrix}, \quad \langle 0| = \begin{pmatrix} 1 & 0 \end{pmatrix}, \quad |1\rangle = \begin{pmatrix} 0 \\ 1 \end{pmatrix}, \quad \langle 1| = \begin{pmatrix} 0 & 1 \end{pmatrix}, \quad \begin{array}{c} \cdot \cdot \cdot \\ \vdots \\ \cdot \cdot \cdot \\ \vdots \\ \cdot \cdot \cdot \end{array}$$

denotes the empty diagram.

**Remark 2.1** If  $\mathcal{R} = \mathbb{C}$ , then the interpretation of the red spider we defined here is just the normal red spider [3] written in terms of computational basis with all the coefficients being 1. To see this, one just need to notice that the red spider can be generated by the monoid pair (and its flipped version)   corresponding to matrices  $\begin{pmatrix} 1 & 0 & 0 & 1 \\ 0 & 1 & 1 & 0 \end{pmatrix}$  and  $\begin{pmatrix} 1 \\ 0 \end{pmatrix}$  respectively, which means the red spider defined in this way is the same as the normal red spider (see e.g. [3]) up to a scalar depending on the number of inputs and outputs of the spider.

For simplicity, we make the following conventions:



Now we give rules for ZX-calculus over  $\mathcal{R}$ .

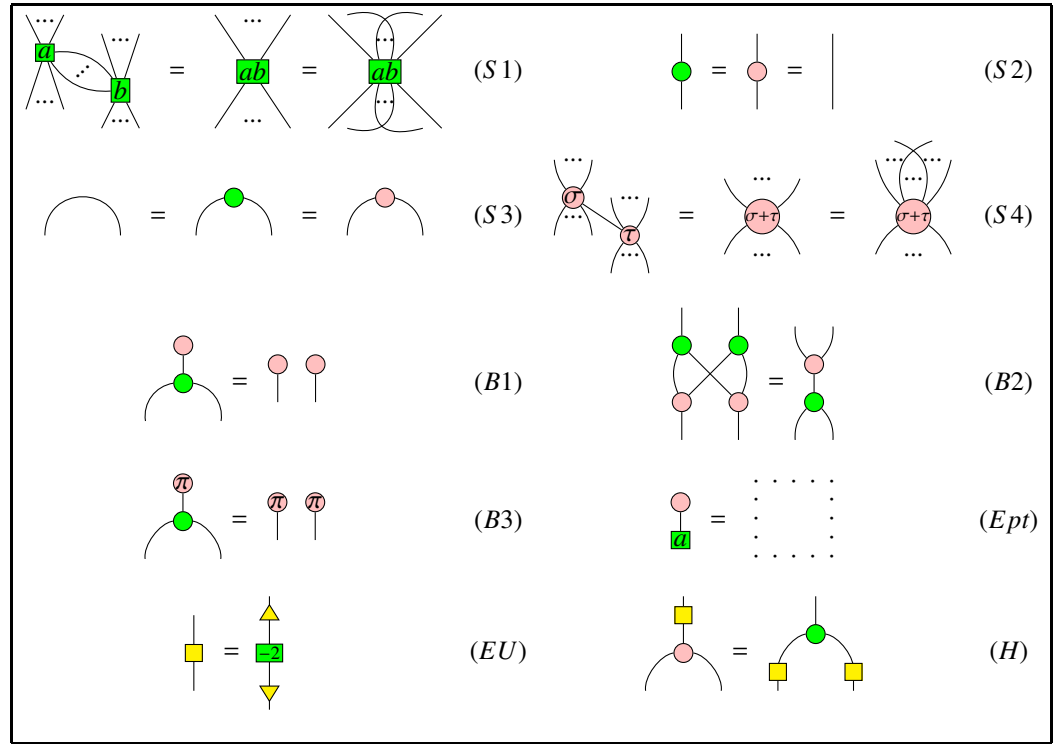
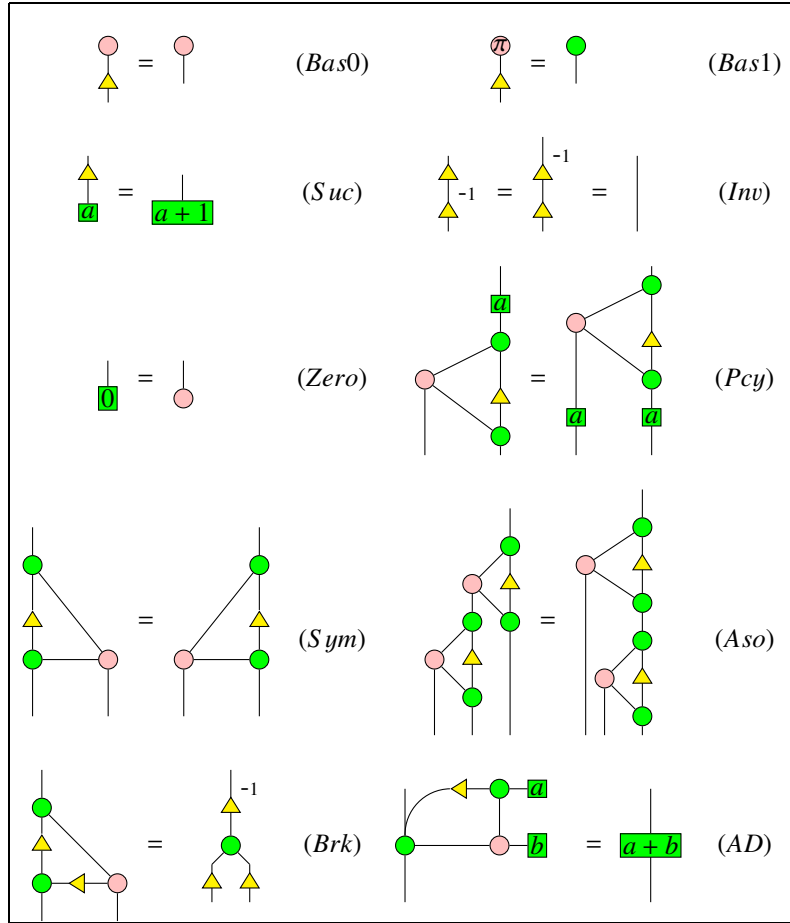


Figure 1: ZX rules I, over an arbitrary commutative ring  $\mathcal{R}$ ,  $a, b \in \mathcal{R}$ ,  $\sigma, \tau \in \{0, \pi\}$ ,  $+$  is a modulo  $2\pi$  addition in (S4). The upside-down flipped versions of the rules are assumed to hold as well.



It is a routine check that these rules are sound in the sense that they still hold under the standard interpretation  $\llbracket \cdot \rrbracket$ .

### 3 Derivable equalities mainly from previous results

In this section, we list equalities from algebraic rules in Figure 1. Some equalities have been essentially derived in [14], we just list them without giving the proof if it still holds in the case of rings. For simplicity, we give two denotations as follows:

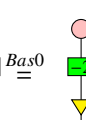
$$\begin{array}{c}
 \text{Diagram 1:} \\
 \text{Left: } \cdots \text{ } \square \text{ } \cdots \text{ } := \text{ } \cdots \text{ } \square \text{ } \cdots \text{ } \text{ (with a green dot at the bottom)} \\
 \text{Middle: } \cdots \text{ } \triangle \text{ } \cdots \text{ } := \text{ } \cdots \text{ } \triangle \text{ } \cdots \text{ } \text{ (with a green dot at the bottom)} \\
 \text{Right: } \cdots \text{ } \triangle \text{ } \cdots \text{ } := \text{ } \cdots \text{ } \square \text{ } \cdots \text{ } \text{ (with a green dot at the bottom)} \\
 \text{ (1)}
 \end{array}$$

Clearly, they have the following relation

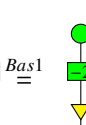
$$\begin{array}{c}
 \text{Diagram 2:} \\
 \cdots \text{ } \triangle \text{ } \cdots = \text{ } \cdots \text{ } \square \text{ } \cdots = \text{ } \cdots \text{ } \square \text{ } \cdots \\
 \text{ (2)}
 \end{array}$$

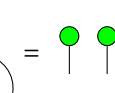
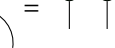
**Lemma 3.1** [13]  = 

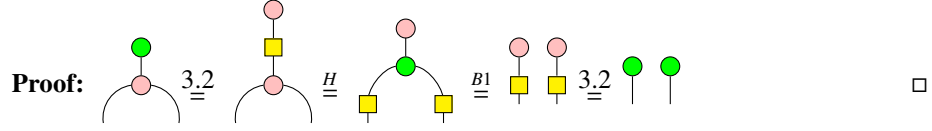
**Lemma 3.2**  = 

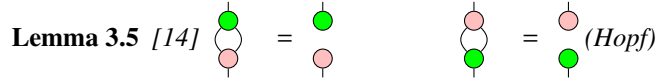
**Proof:**   $\stackrel{Eu}{=} \text{ } \square \text{ } \stackrel{Bas0}{=} \text{ } \square \text{ } \stackrel{S1}{=} \text{ } \square \text{ } \stackrel{B1}{=} \text{ } \square \text{ } \stackrel{3.1}{\stackrel{Ept}{=}} \text{ } \square \text{ } \quad \square$

**Lemma 3.3**  = 

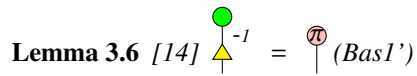
**Proof:**   $\stackrel{Eu}{=} \text{ } \square \text{ } \stackrel{Bas1}{=} \text{ } \square \text{ } \stackrel{S1}{=} \text{ } \square \text{ } \stackrel{Suc}{=} \text{ } \square \text{ } = \text{ } \square \text{ } \quad \square$

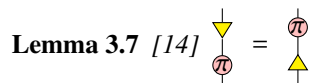
**Lemma 3.4**  = 

**Proof:** 

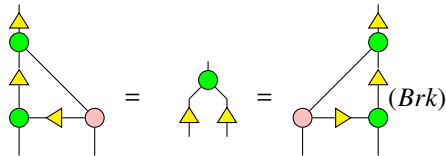
**Lemma 3.5 [14]** 

The first equality is proved in [14] which is also valid here. The second equality follows from the first one by taking transpose on both sides.

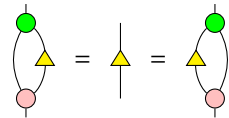
**Lemma 3.6 [14]** 

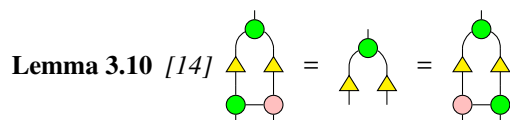
**Lemma 3.7 [14]** 

**Lemma 3.8 [14]**

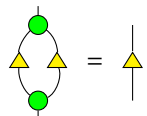


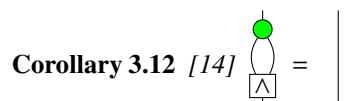
**Lemma 3.9 [14]**



**Lemma 3.10 [14]** 

**Lemma 3.11 [14]**



**Corollary 3.12 [14]** 

**Lemma 3.13** [14]

$$\begin{array}{c} \text{Diagram 1} \\ \text{Diagram 2} \end{array} = \boxed{\quad} = \begin{array}{c} \text{Diagram 3} \\ \text{Diagram 4} \end{array} \quad (3)$$

**Lemma 3.14** [14]

$$\begin{array}{c} \text{Diagram 1} \\ \text{Diagram 2} \end{array} = \boxed{\quad} = \begin{array}{c} \text{Diagram 3} \\ \text{Diagram 4} \end{array} \quad (4)$$

**Lemma 3.15** [1]  $\boxed{\quad} = \begin{array}{c} \text{Diagram 1} \\ \text{Diagram 2} \end{array}$

**Lemma 3.16**  $\boxed{\quad} = \begin{array}{c} \text{Diagram 1} \\ \text{Diagram 2} \end{array} \quad (B3)$

**Proof:**

$$\begin{array}{c} \text{Diagram 1} \\ \text{Diagram 2} \end{array} \stackrel{3.3}{=} \boxed{\quad} \stackrel{H}{=} \begin{array}{c} \text{Diagram 3} \\ \text{Diagram 4} \end{array} \stackrel{B3}{=} \begin{array}{c} \text{Diagram 5} \\ \text{Diagram 6} \end{array} \stackrel{3.3}{=} \begin{array}{c} \text{Diagram 7} \\ \text{Diagram 8} \end{array}$$

We also call this equality (B3).  $\square$

**Lemma 3.17** [14] Suppose  $m \geq 0$ . Then

$$\begin{array}{c} \text{Diagram 1} \\ \text{Diagram 2} \end{array} = \begin{array}{c} \text{Diagram 3} \\ \text{Diagram 4} \end{array} \quad (\text{Pic})$$

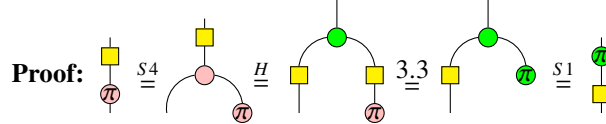
**Proof:**

$$\begin{array}{c} \text{Diagram 1} \\ \text{Diagram 2} \end{array} \stackrel{3.15}{=} \boxed{\quad} \stackrel{B1}{=} \begin{array}{c} \text{Diagram 3} \\ \text{Diagram 4} \end{array} \stackrel{3.2}{=} \begin{array}{c} \text{Diagram 5} \\ \text{Diagram 6} \end{array} \stackrel{Ept}{=} \begin{array}{c} \text{Diagram 7} \\ \text{Diagram 8} \end{array}$$

$$\begin{array}{c} \text{Diagram 1} \\ \text{Diagram 2} \end{array} \stackrel{S1}{=} \begin{array}{c} \text{Diagram 3} \\ \text{Diagram 4} \end{array} \stackrel{B2}{=} \begin{array}{c} \text{Diagram 5} \\ \text{Diagram 6} \end{array} \stackrel{B3}{=} \begin{array}{c} \text{Diagram 7} \\ \text{Diagram 8} \end{array} \stackrel{S1}{=} \begin{array}{c} \text{Diagram 9} \\ \text{Diagram 10} \end{array}$$

The general case follows directly from the above two special cases.  $\square$

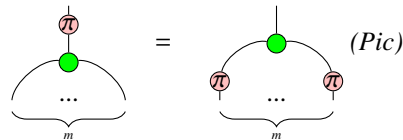
**Lemma 3.18** 

**Proof:**   $\square$

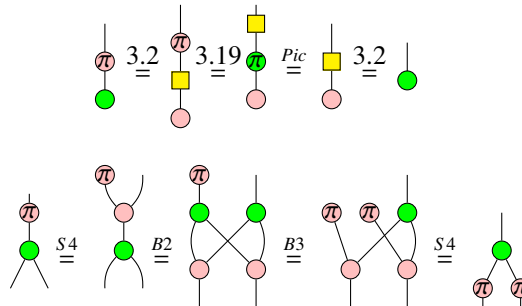
**Corollary 3.19** 

**Proof:** This can be obtained from lemma 3.18 by transpose on both sides.  $\square$

**Lemma 3.20** [14] Suppose  $m \geq 0$ . Then

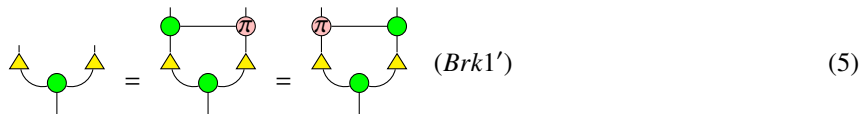


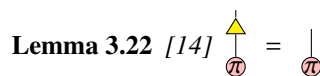
**Proof:**

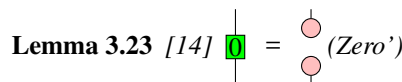


The general case follows directly from the above two special cases. We also call this equality (Pic) for convenience.  $\square$

**Corollary 3.21** [14]



**Lemma 3.22** [14] 

**Lemma 3.23** [14] 

**Lemma 3.24** [14]

The diagram shows three configurations of a loop with two nodes: a green node at the top and a red node at the bottom. The loop has two yellow arrows pointing clockwise. The first configuration has the green node on the left and the red node on the right. The second configuration has the green node at the top and the red node at the bottom, with the loop being a vertical line. The third configuration has the green node on the right and the red node on the left. All three configurations are connected by equals signs.

**Lemma 3.25** [14]

The diagram shows a loop with a green node at the top and a red node at the bottom. A yellow arrow points clockwise around the loop. This is followed by an equals sign and a red node with a yellow arrow pointing downwards.

**Lemma 3.26** [14]

The diagram shows a loop with a green node at the top and a red node at the bottom. A yellow arrow points clockwise around the loop. This is followed by an equals sign and a red node with a yellow arrow pointing downwards.

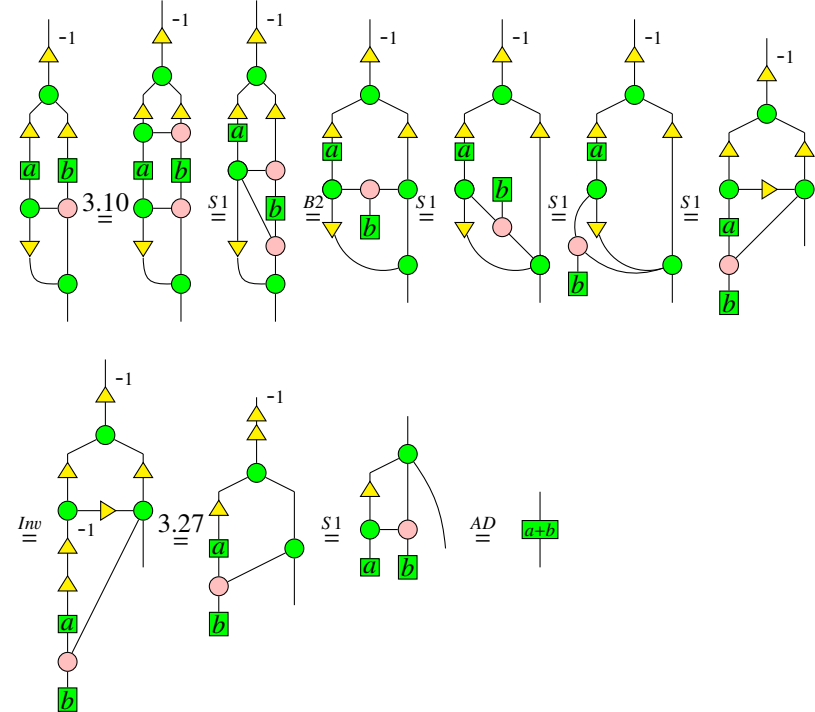
**Lemma 3.27** [14]

The diagram shows three configurations of a loop with two nodes: a green node at the top and a red node at the bottom. The loop has two yellow arrows pointing clockwise. The first configuration has the green node on the left and the red node on the right. The second configuration has the green node at the top and the red node at the bottom, with the loop being a vertical line. The third configuration has the green node on the right and the red node on the left. The bottom configuration has a superscript  $-1$  to its right. All three configurations are connected by equals signs.

**Lemma 3.28** [14]

The diagram shows a complex loop structure. It starts with a red node at the top, followed by a green node. A yellow arrow points down to a red node, which is then connected to a green node. From this green node, a yellow arrow points up to a green node at the top. A yellow arrow also points down from this green node to a red node. This structure is followed by an equals sign and a red node with a yellow arrow pointing upwards. To the right of this red node is the expression  $(AD')$ .

## Proof:



□

**Lemma 3.29** [14]  =  (Ivt)

**Lemma 3.30** [14]  $\pi = \pi \otimes \pi$

**Lemma 3.31** [14]  = 

**Corollary 3.32 [14]**

$$\text{Diagram 6: } \text{Diagram 1} = \text{Diagram 2} \quad (6)$$

$$\text{Lemma 3.33 [14]} \quad \text{Diagram: } \begin{array}{c} \text{A green circle with a yellow arrow pointing to it from the left, and a yellow arrow pointing away from it to the right.} \\ = \\ \text{A green circle with a yellow arrow pointing to it from the left, and a yellow arrow pointing away from it to the right.} \end{array}$$

**Lemma 3.34 [14]**

$$\text{Diagram: } \begin{array}{c} \text{A green circle with a yellow arrow pointing to it from the left, and a yellow arrow pointing away from it to the right.} \\ = \\ \text{A green circle with a yellow arrow pointing to it from the left, and a yellow arrow pointing away from it to the right.} \end{array} \quad (7)$$

$$\text{Lemma 3.35 [14]} \quad \text{Diagram: } \begin{array}{c} \text{A green circle with a yellow arrow pointing to it from the left, and a yellow arrow pointing away from it to the right.} \\ = \\ \text{A green circle with a yellow arrow pointing to it from the left, and a yellow arrow pointing away from it to the right.} \end{array}$$

$$\text{Lemma 3.36 [14]} \quad \text{Diagram: } \begin{array}{c} \text{A green circle with a yellow arrow pointing to it from the left, and a yellow arrow pointing away from it to the right.} \\ = \\ \text{A green circle with a yellow arrow pointing to it from the left, and a yellow arrow pointing away from it to the right.} \end{array} \quad (\text{Brkp})$$

$$\text{Lemma 3.37 [14]} \quad \text{Diagram: } \begin{array}{c} \text{A green circle with a yellow arrow pointing to it from the left, and a yellow arrow pointing away from it to the right.} \\ = \\ \text{A green circle with a yellow arrow pointing to it from the left, and a yellow arrow pointing away from it to the right.} \end{array} \quad (\text{BiA})$$

$$\text{Corollary 3.38 [14]} \quad \text{Diagram: } \begin{array}{c} \text{A green circle with a yellow arrow pointing to it from the left, and a yellow arrow pointing away from it to the right.} \\ = \\ \text{A green circle with a yellow arrow pointing to it from the left, and a yellow arrow pointing away from it to the right.} \end{array}$$

**Corollary 3.39 [14]** For any  $k \geq 0$ , we have

$$\text{Diagram: } \begin{array}{c} \text{A green circle with a yellow arrow pointing to it from the left, and a yellow arrow pointing away from it to the right.} \\ = \\ \text{A green circle with a yellow arrow pointing to it from the left, and a yellow arrow pointing away from it to the right.} \end{array}$$

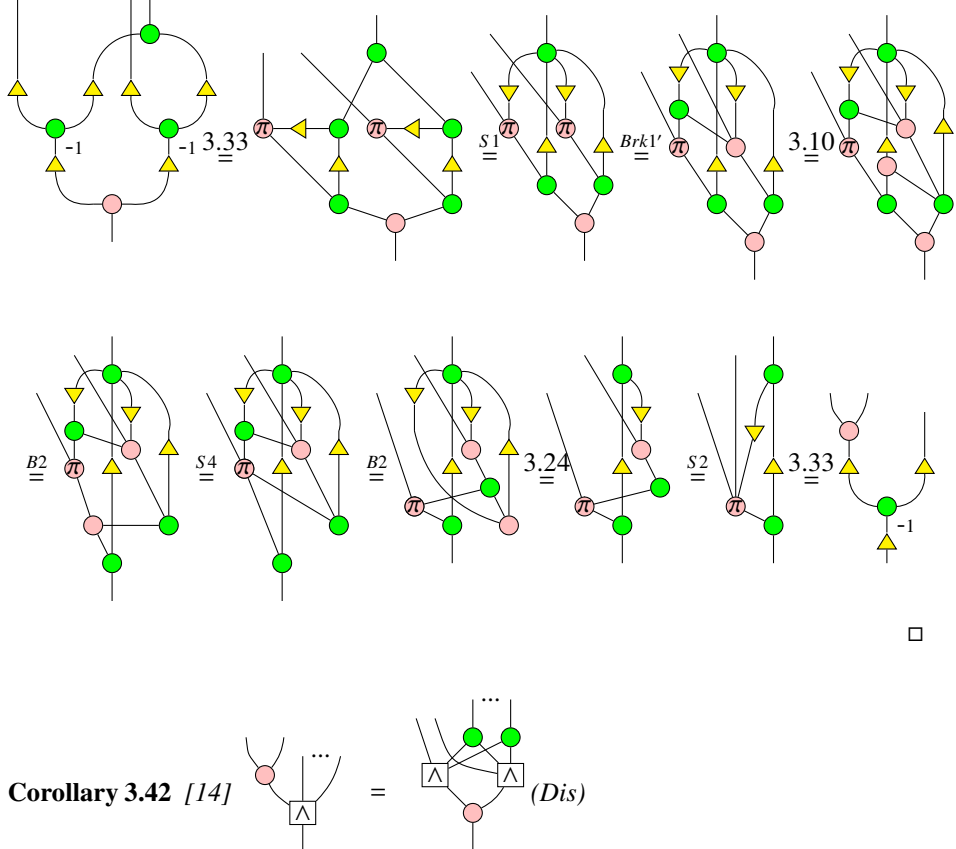
or equivalently,

where

**Corollary 3.40** [14]

**Lemma 3.41** [14]

**Proof:**

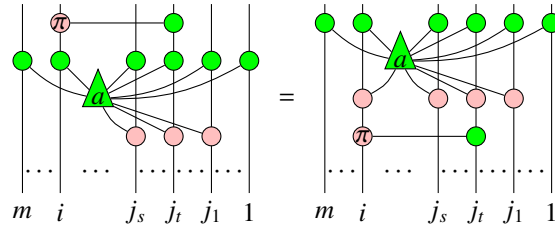


This follows directly from Corollary 3.39 and Lemma 3.41. We also call this equality (Dis) for convenience.

## 4 Newly derivable equalities

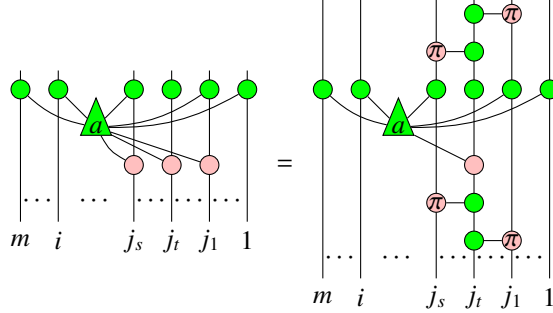
In this section, we derive all the equalities needed for the proof of completeness while relatively new to previous results.

**Proposition 4.1** [14] *Let  $i, j_1, \dots, j_t, \dots, j_s \in \{1, \dots, m\}$ ,  $i \notin \{j_1, \dots, j_t, \dots, j_s\}$ . Then we have*

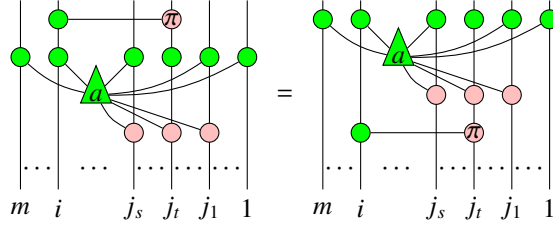


where the node  $a$  is connected to  $j_1, \dots, j_t, \dots, j_s$  via pink nodes.

**Corollary 4.2** [14]



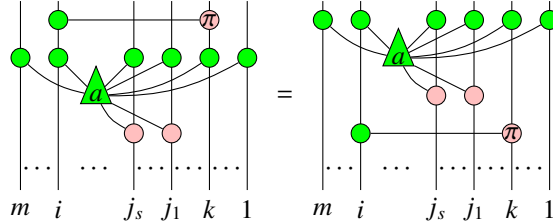
**Proposition 4.3** [14] Let  $i, j_1, \dots, j_t, \dots, j_s \in \{1, \dots, m\}$ ,  $i \notin \{j_1, \dots, j_t, \dots, j_s\}$ . Then we have



where the node  $a$  is connected to  $j_1, \dots, j_t, \dots, j_s$  via pink nodes.

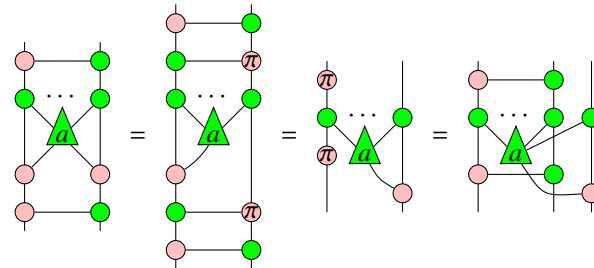
Similarly, we have

**Proposition 4.4** [14] Let  $i, k, j_1, \dots, j_s \in \{1, \dots, m\}$ ,  $i, k \notin \{j_1, \dots, j_s\}$ . Then we have



where the node  $a$  is connected to  $j_1, \dots, j_s$  via pink nodes.

**Corollary 4.5** [14]



In the same way, we have

### **Proposition 4.6 [14]**

$$\begin{array}{c} \text{Diagram 1:} \\ \text{A circuit with two green nodes on the left, a red node at the top, and a blue node in the center. The blue node is connected to the top red node and to two green nodes below it. The bottom green nodes are connected to each other. The entire structure is enclosed in a box labeled 'A'.} \\ = \\ \begin{array}{c} \text{Diagram 2:} \\ \text{A circuit with two green nodes on the left, a red node at the top, and a blue node in the center. The blue node is connected to the top red node and to two green nodes below it. The bottom green nodes are connected to each other. The entire structure is enclosed in a box labeled 'A'.} \end{array} \end{array}$$

**Corollary 4.7 [14]**

$$\begin{array}{c} \text{Diagram 1:} \\ \text{A circuit with 5 nodes. The top and bottom nodes are pink. The middle row has two green nodes. The left green node is connected to the top and bottom nodes. The right green node is connected to the top and bottom nodes. A box labeled 'A' is connected to the top and bottom nodes. A box labeled 'a' is connected to the left green node and the box 'A'.} \\ = \\ \text{Diagram 2:} \\ \text{A circuit with 5 nodes. The top and bottom nodes are pink. The middle row has two green nodes. The left green node is connected to the top and bottom nodes. The right green node is connected to the top and bottom nodes. A box labeled 'A' is connected to the top and bottom nodes. A box labeled 'a' is connected to the left green node and the box 'A'. The right green node is connected to a box labeled 'π'.} \end{array}$$

**Lemma 4.8** [14]

$$\begin{array}{c}
 \text{Diagram:} \\
 \text{A directed graph with 6 nodes. Nodes 1, 2, 3, and 4 are green circles, while nodes 5 and 6 are pink circles. Directed edges: } \\
 \begin{aligned}
 &1 \rightarrow 2, \quad 1 \rightarrow 3, \\
 &2 \rightarrow 4, \quad 3 \rightarrow 4, \\
 &4 \rightarrow 5, \quad 4 \rightarrow 6, \\
 &5 \rightarrow 6, \\
 &6 \rightarrow 1. 
 \end{aligned}
 \end{array}
 = \begin{array}{c}
 \text{Diagram:} \\
 \text{A directed graph with 2 nodes, both green circles. Directed edges: } \\
 \begin{aligned}
 &1 \rightarrow 2, \\
 &2 \rightarrow 1.
 \end{aligned}
 \end{array}$$

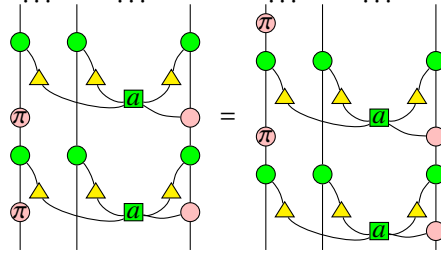
**Lemma 4.9 [14]**

$$\begin{array}{c} \text{Diagram 1} \\ \text{Diagram 2} \end{array} = \begin{array}{c} \text{Diagram 3} \\ \text{Diagram 4} \end{array}$$

**Proposition 4.10** [14] For any  $k \geq 1$ , we have

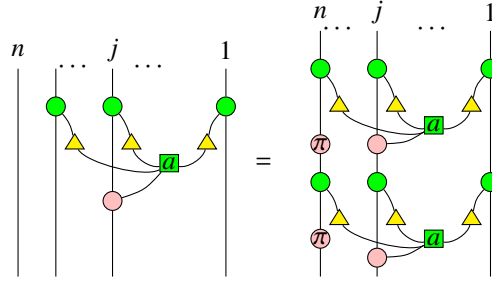
$$\begin{array}{c} \text{Diagram 1} \\ \text{Diagram 2} \end{array} = \begin{array}{c} \text{Diagram 3} \\ \text{Diagram 4} \end{array} \quad (8)$$

**Corollary 4.11** [14]



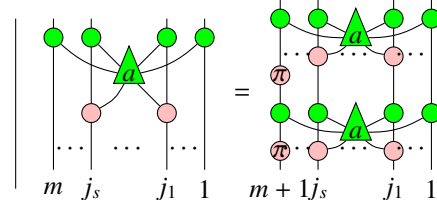
This can be immediately obtained by plugging pink  $\pi$  phase gates from the top and the bottom of the left-most line of diagrams on both sides of (8).

**Corollary 4.12** [14]



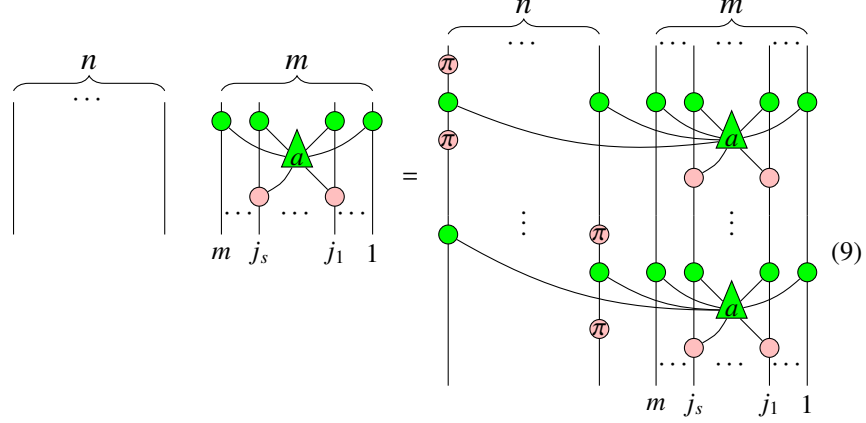
This can be obtained by swapping the 1-th and the  $j$ -th lines of diagrams on both side of (8).

**Corollary 4.13** [14]



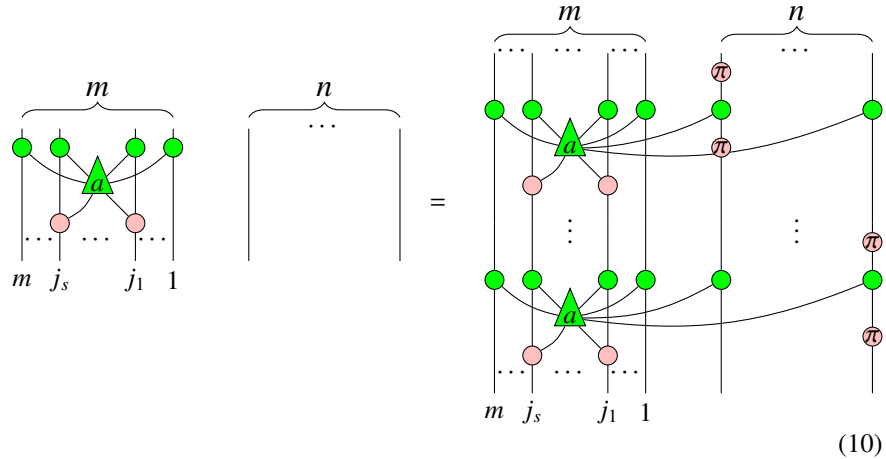
This follows directly from Proposition 4.10 and Corollary 4.2.

**Corollary 4.14** [14]



where on the RHD of (9), there are  $2^n$  green triangles labeled by  $a$  on the right-most  $m$  wires, each green triangle is connected to the left-most  $n$  wires via green dots which are surrounded by  $k$  pairs of red  $\pi$ s with  $0 \leq k \leq n$ , and different green triangles have different distribution of pairs of red  $\pi$ s, that's why there are  $\binom{n}{0} + \binom{n}{1} + \dots + \binom{n}{n} = 2^n$  green triangles labeled by  $a$ .

**Corollary 4.15** [14]



where on the RHD of (9), there are  $2^n$  green triangles labeled by  $a$  on the left-most  $m$  wires, each green triangle is connected to the right-most  $n$  wires via green dots which are surrounded by  $k$  pairs of red  $\pi$ s with  $0 \leq k \leq n$ , and different green triangles have different distribution of pairs of red  $\pi$ s, that's why there are  $\binom{n}{0} + \binom{n}{1} + \dots + \binom{n}{n} = 2^n$  green triangles labeled by  $a$ .

**Proposition 4.16** [14] For any  $k \geq 1$ , we have

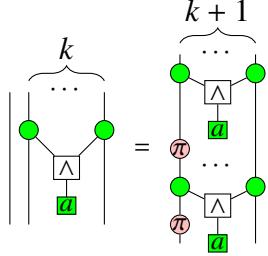
**Corollary 4.17** [14]

This can be directly obtained from Proposition 4.16 and Corollary 4.2.

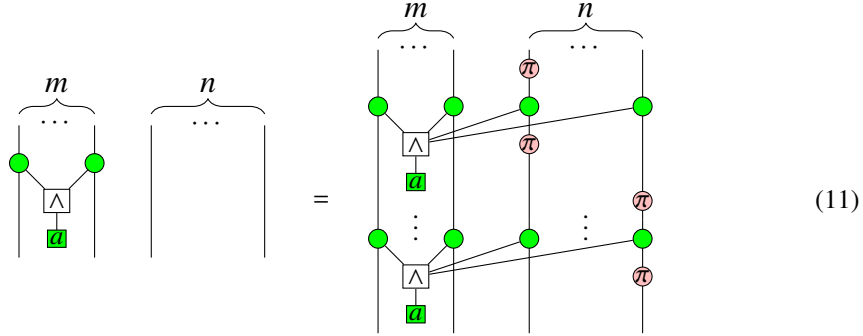
**Lemma 4.18** [14]

**Lemma 4.19** [14]

**Proposition 4.20** [14] For any  $k \geq 1$ , we have

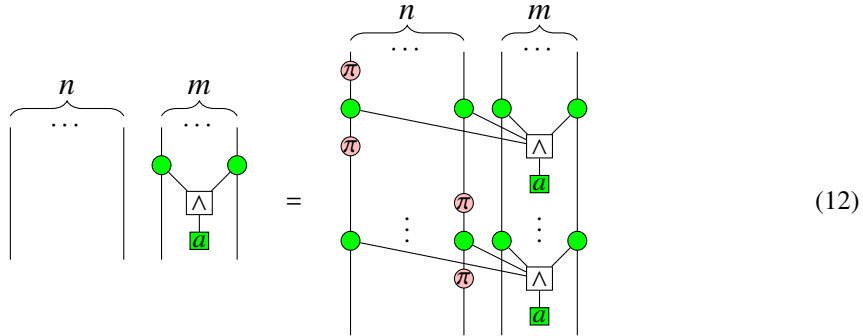


**Corollary 4.21** [14]

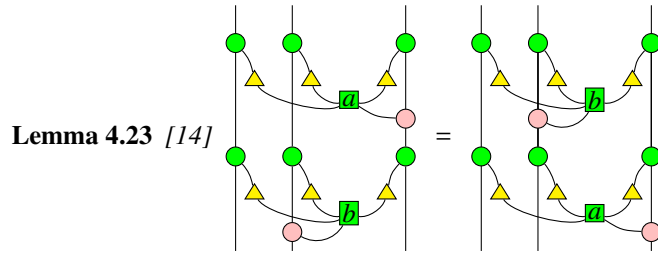


where on the RHD of (11), there are  $2^n$  AND gates on the left-most  $m$  wires, each AND gate is accompanied by  $k$  pairs of red  $\pi$ s on the left-most  $n$  wires with  $0 \leq k \leq n$ , and different AND gates have different distribution of pairs of red  $\pi$ s, that's why there are  $\binom{n}{0} + \binom{n}{1} + \dots + \binom{n}{n} = 2^n$  AND gates.

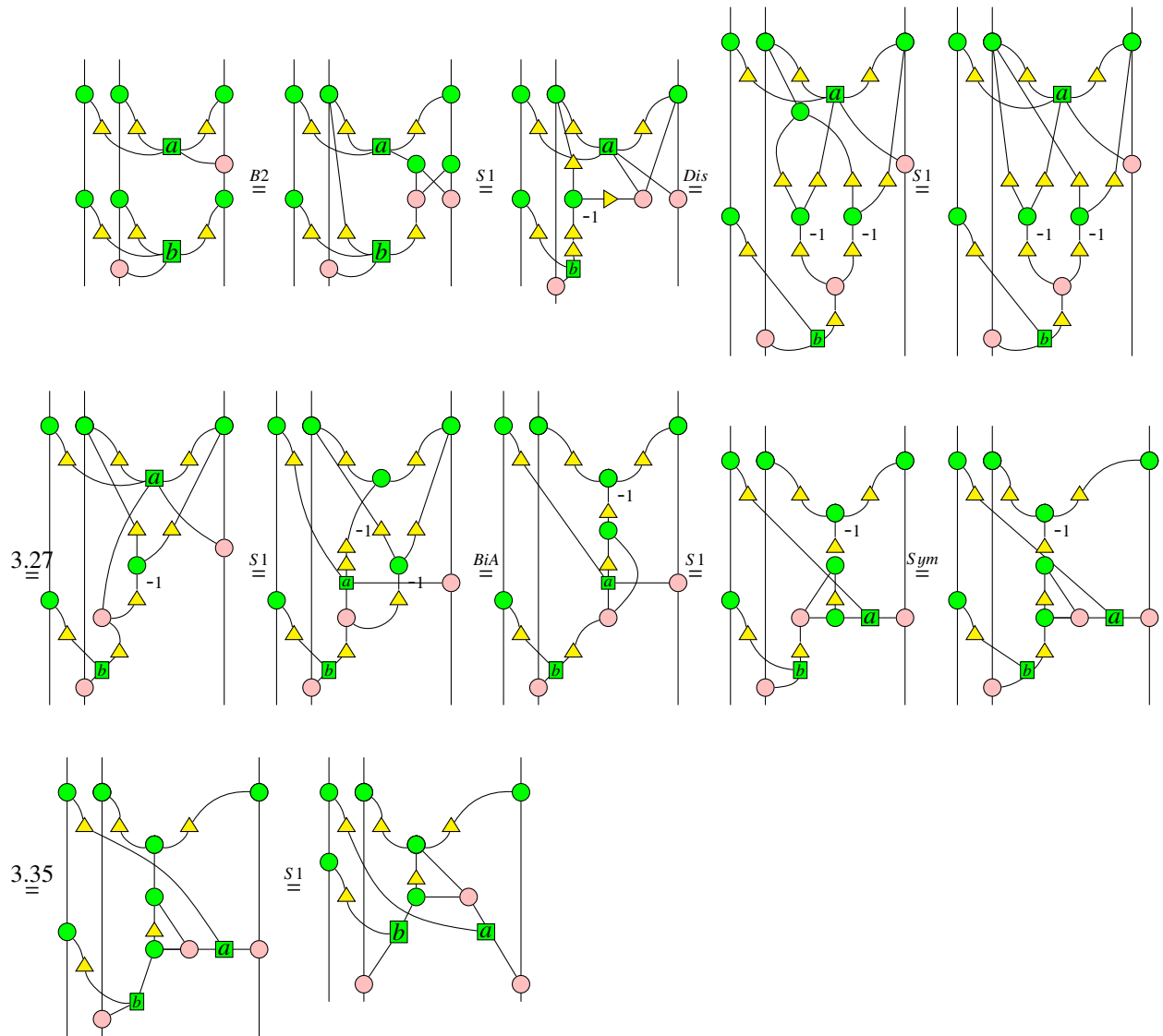
**Corollary 4.22** [14]

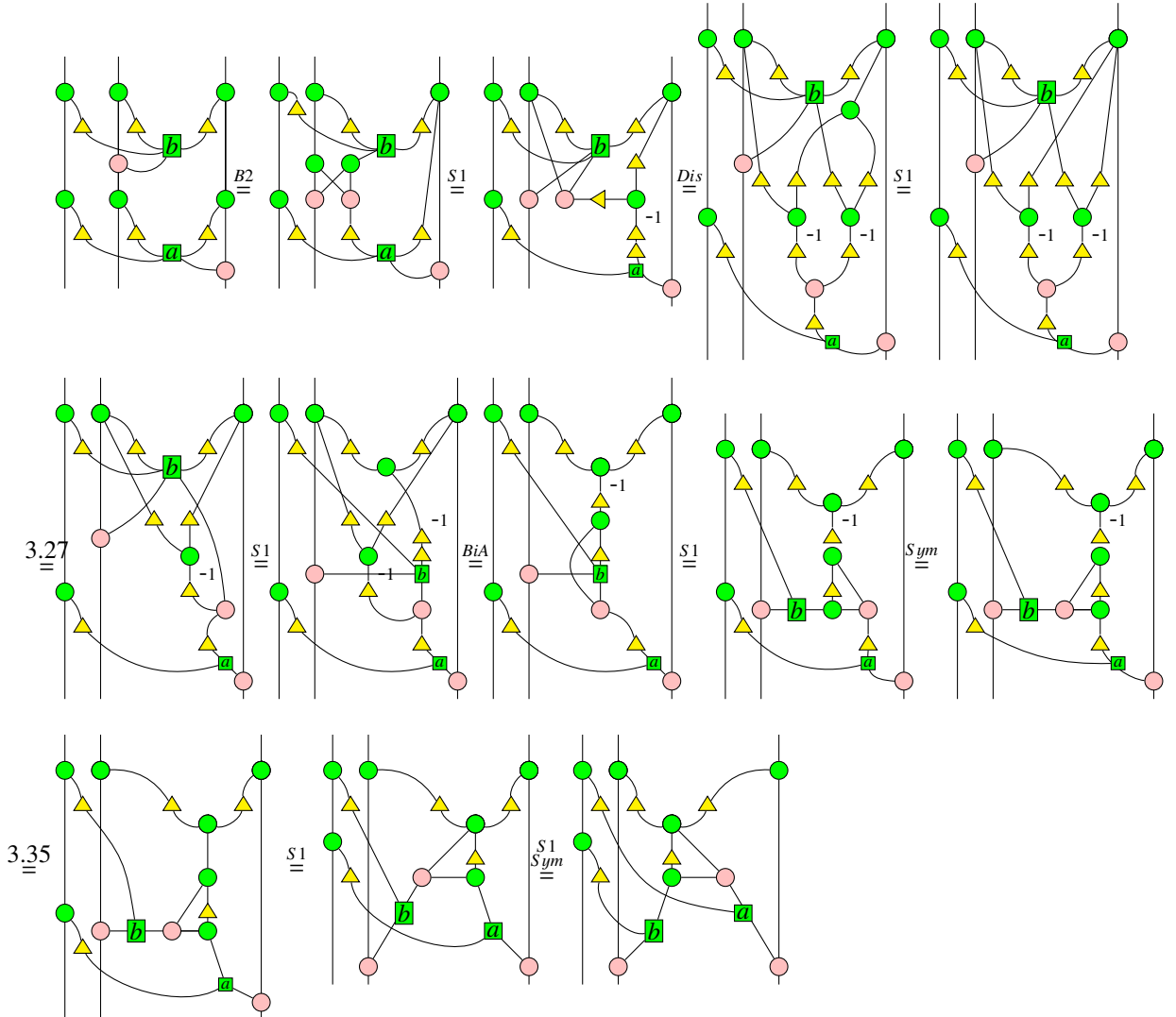


where on the RHD of (12), there are  $2^n$  AND gates on the right-most  $m$  wires, each AND gate is accompanied by  $k$  pairs of red  $\pi$ s on the left-most  $n$  wires with  $0 \leq k \leq n$ , and different AND gates have different distribution of pairs of red  $\pi$ s, that's why there are  $\binom{n}{0} + \binom{n}{1} + \dots + \binom{n}{n} = 2^n$  AND gates.

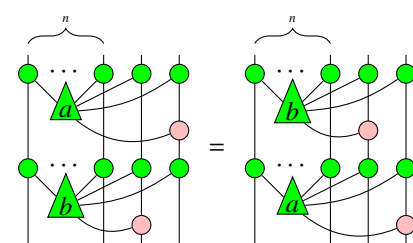


**Proof:**





**Proposition 4.24** [14] Let  $n \geq 0$ . Then we have

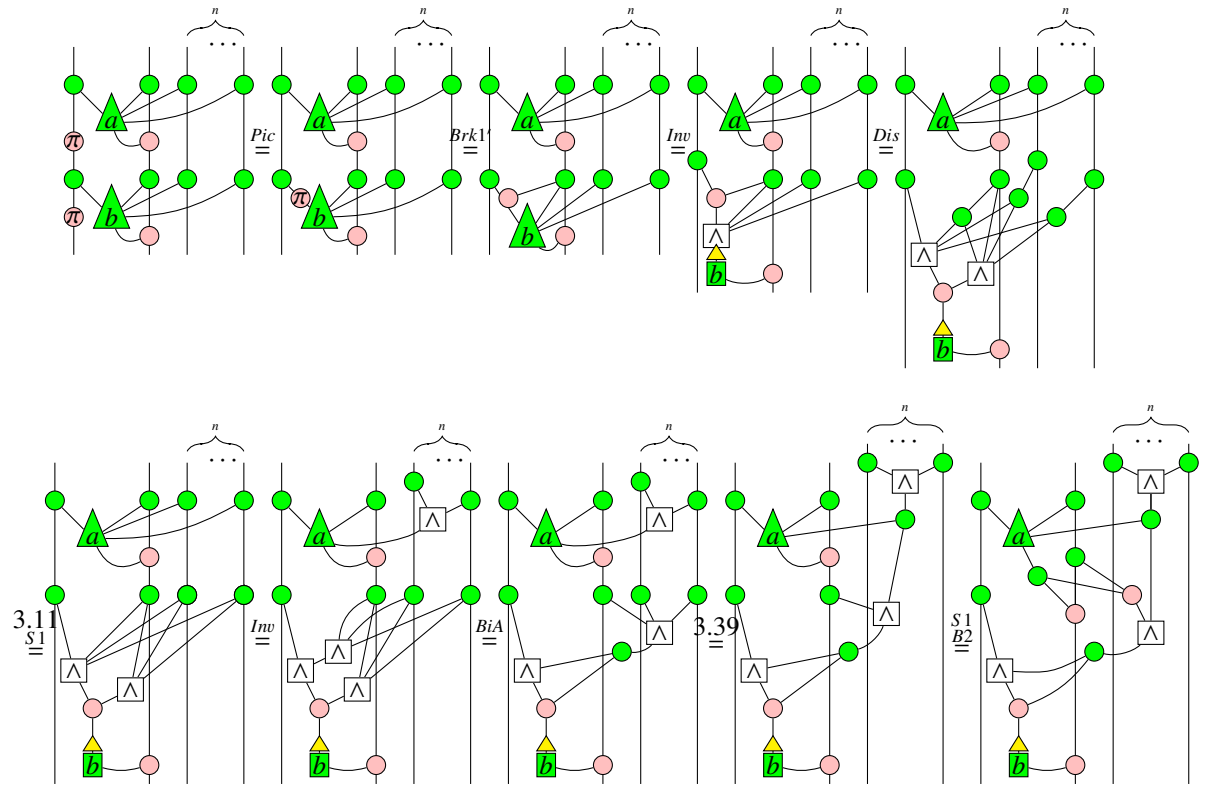


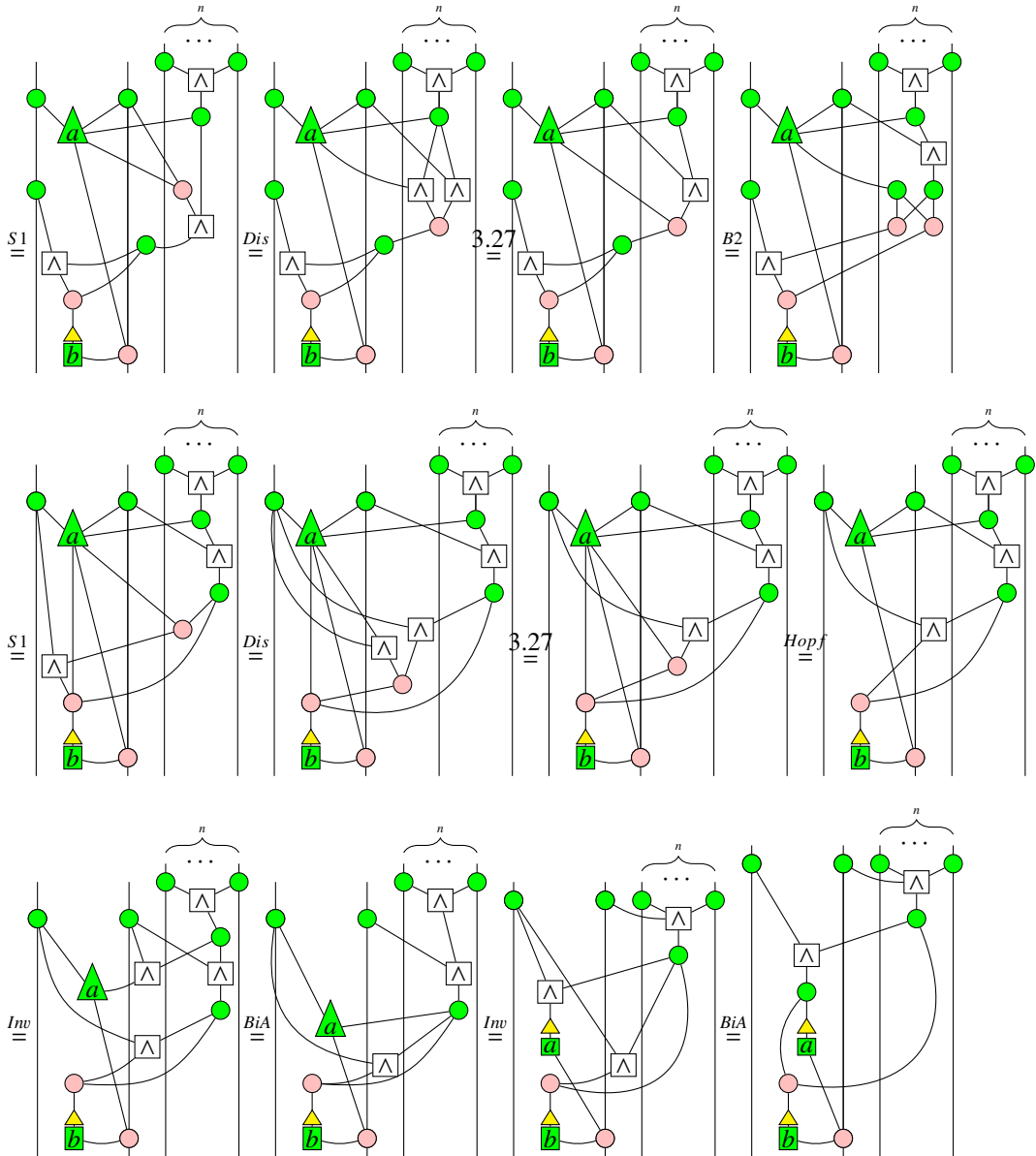
**Proposition 4.25** [14] Assume that node  $a$  is connected to  $j_1, \dots, j_s$  via pink nodes and node  $b$  is connected to  $i_1, \dots, i_t$  via pink nodes, where  $i_1, \dots, i_t, j_1, \dots, j_s \in \{1, \dots, m\}$ , and  $\{i_1, \dots, i_t\} \neq \emptyset, \{j_1, \dots, j_s\} \neq \emptyset$ . Then we have

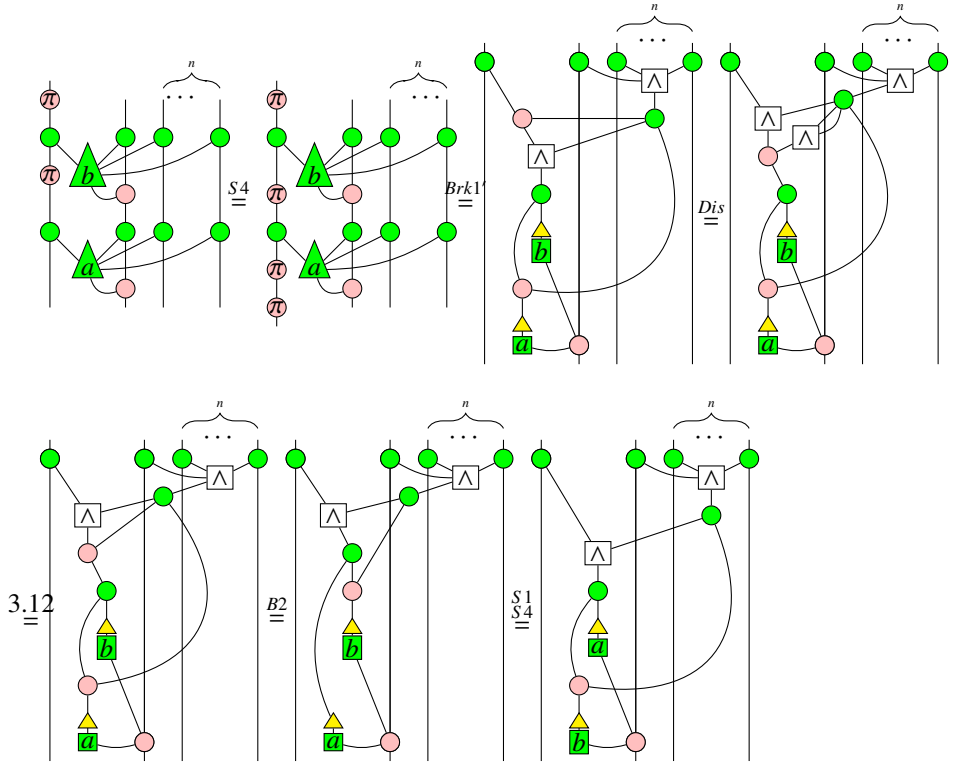
(13)

**Proposition 4.26** [14] Assume that  $n \geq 0$ . Then

**Proof:**

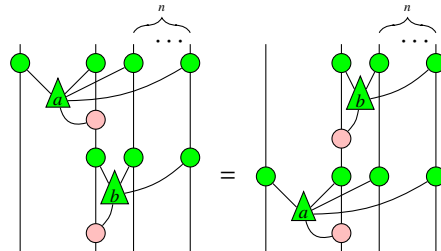




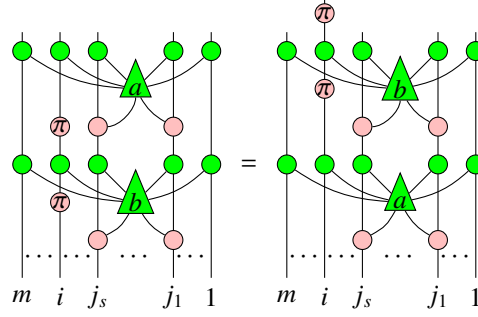


□

**Corollary 4.27** [14] Assume that  $n \geq 0$ . Then

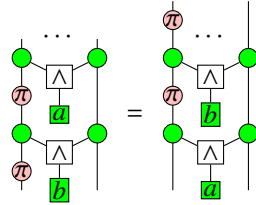


**Corollary 4.28** [14]

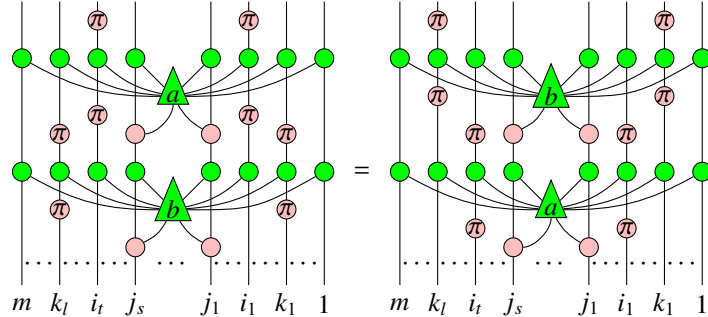


where the node  $a$  and  $b$  are connected to  $j_1, \dots, j_s$  via pink nodes, and two red  $\pi$  nodes are located on the  $i$ -th line,  $i \notin \{j_1, \dots, j_s\}$  or  $i \in \{j_1, \dots, j_s\}$ ,  $|\{j_1, \dots, j_s\}| \geq 2$ .

**Proposition 4.29** [14]



**Proposition 4.30** [14] Suppose the nodes  $a$  and  $b$  are connected to  $j_1, \dots, j_s$  via pink nodes, pairs of red  $\pi$  nodes separated by green nodes connected to  $a$  are located on  $i_1, \dots, i_t$ , and pairs of red  $\pi$  nodes separated by green nodes connected to  $b$  are located on  $k_1, \dots, k_l$ ,  $\{i_1, \dots, i_t\} \cap \{j_1, \dots, j_s\} = \emptyset$ ,  $\{k_1, \dots, k_l\} \cap \{j_1, \dots, j_s\} = \emptyset$ . Then we have

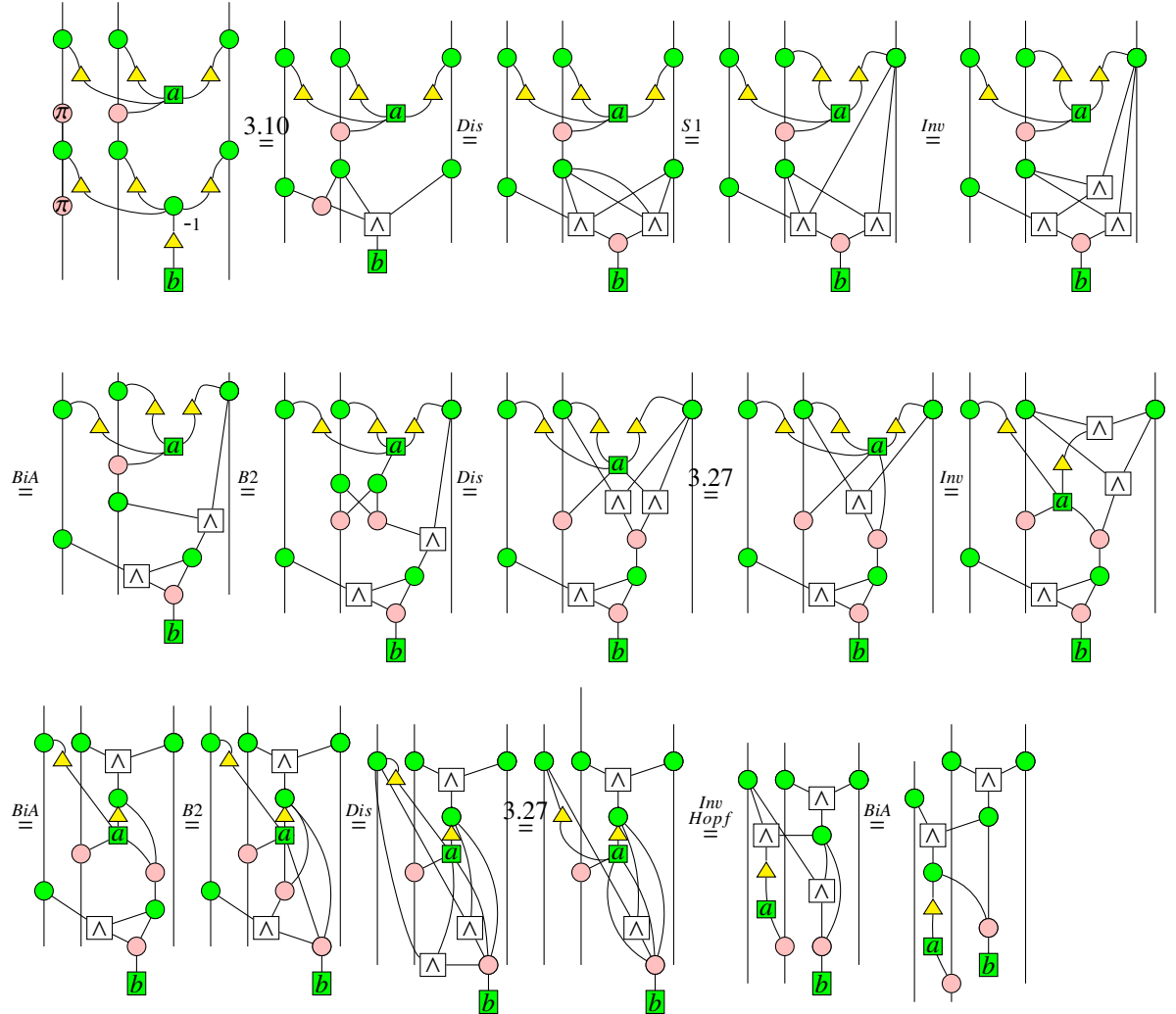


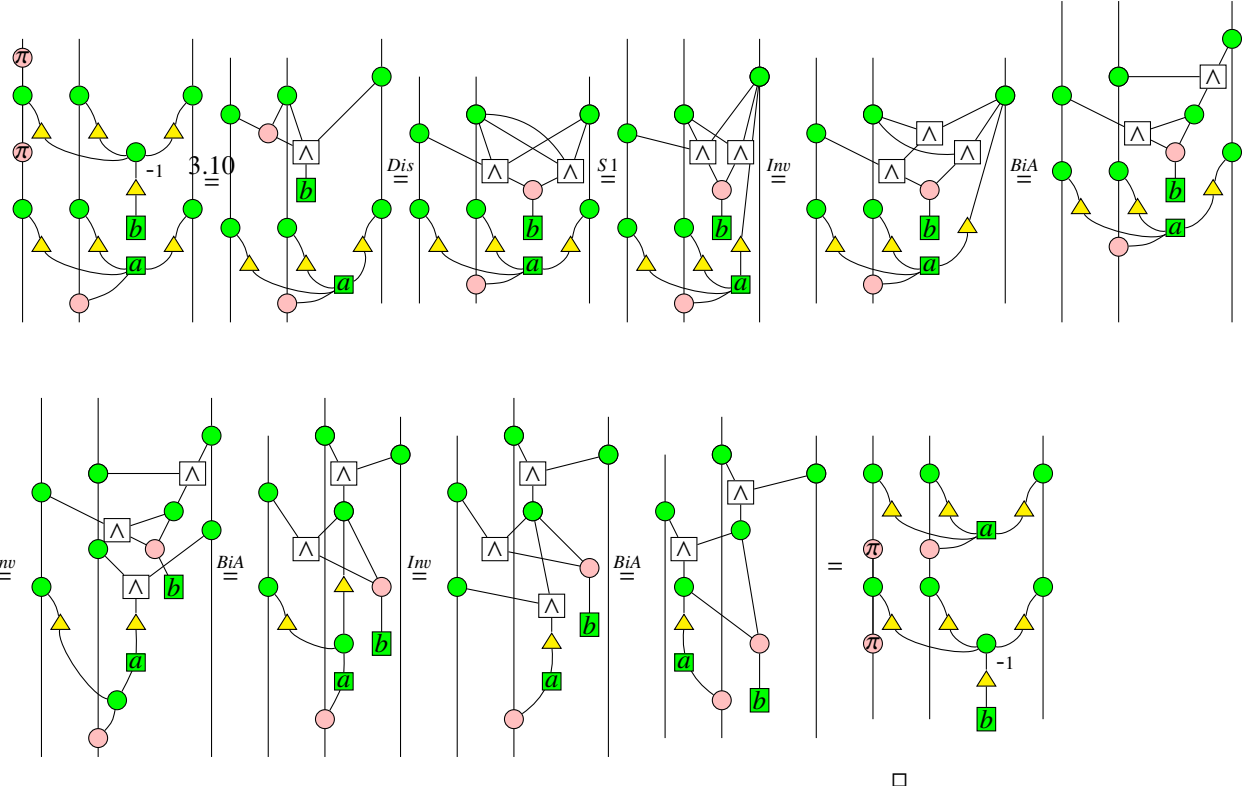
**Proposition 4.31** [14] Suppose the pairs of red  $\pi$  nodes separated by green nodes connected to  $a$  are located on  $i_1, \dots, i_t$ , and pairs of red  $\pi$  nodes separated by green

nodes connected to  $b$  are located on  $j_1, \dots, j_s$ . Then we have

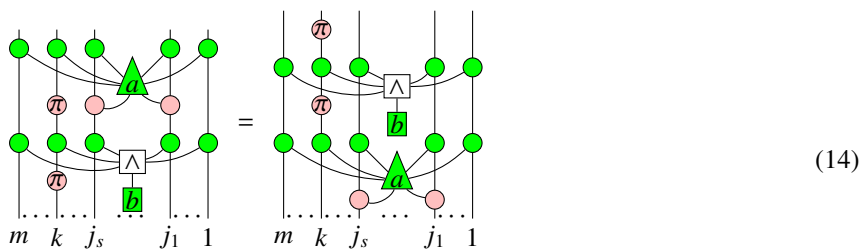
**Proposition 4.32 [14]**

**Proof:**





**Proposition 4.33** [14] Suppose the node  $a$  is connected to  $j_1, \dots, j_s$  via pink nodes, and a pair of red  $\pi$  nodes separated by green nodes connected to  $b$  are located on  $k$ , where  $k \notin \{j_1, \dots, j_s\}$ ,  $|\{j_1, \dots, j_s\}| \geq 1$ , or  $k \in \{j_1, \dots, j_s\}$ ,  $|\{j_1, \dots, j_s\}| \geq 2$ . Then we have



**Proposition 4.34** [14] Suppose the node  $a$  is connected to  $j_1, \dots, j_s$  via pink nodes, pairs of red  $\pi$  nodes separated by green nodes connected to  $a$  are located on  $i_1, \dots, i_t$ , and pairs of red  $\pi$  nodes separated by green nodes connected to  $b$  are located on  $k_1, \dots, k_l$ ,  $\{i_1, \dots, i_t\} \neq \{k_1, \dots, k_l\}$ . Either  $\{k_1, \dots, k_l\} \neq \emptyset$ ,  $\{k_1, \dots, k_l\} \cap \{j_1, \dots, j_s\} = \emptyset$ ,  $|\{j_1, \dots, j_s\}| \geq 1$ ; or  $\{k_1, \dots, k_l\} \neq \emptyset$ ,  $|\{k_1, \dots, k_l\} \cap \{j_1, \dots, j_s\}| = 1$ ,  $|\{j_1, \dots, j_s\}| \geq 2$ ; or symmetrically,  $\{i_1, \dots, i_t\} \neq \emptyset$ ,  $\{i_1, \dots, i_t\} \cap \{j_1, \dots, j_s\} = \emptyset$ ,  $|\{j_1, \dots, j_s\}| \geq 1$ ; or  $\{i_1, \dots, i_t\} \neq \emptyset$ ,  $|\{i_1, \dots, i_t\} \cap \{j_1, \dots, j_s\}| = 1$ ,  $|\{j_1, \dots, j_s\}| \geq 2$ .

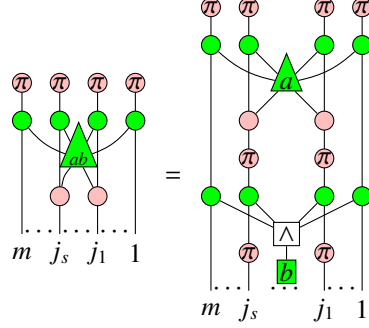
Then we have

**Proposition 4.35 [14]**

**Proof:**

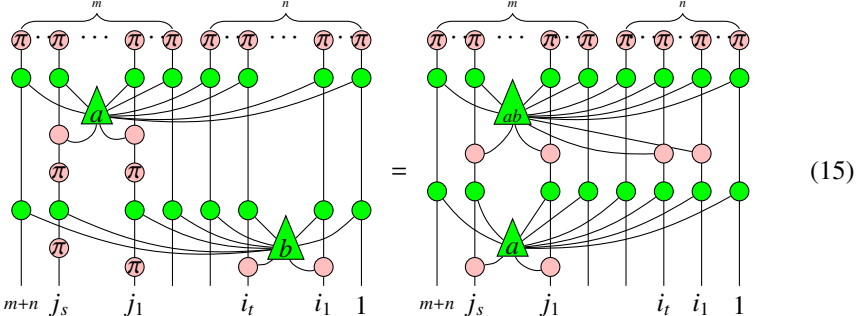
□

**Proposition 4.36** [14]

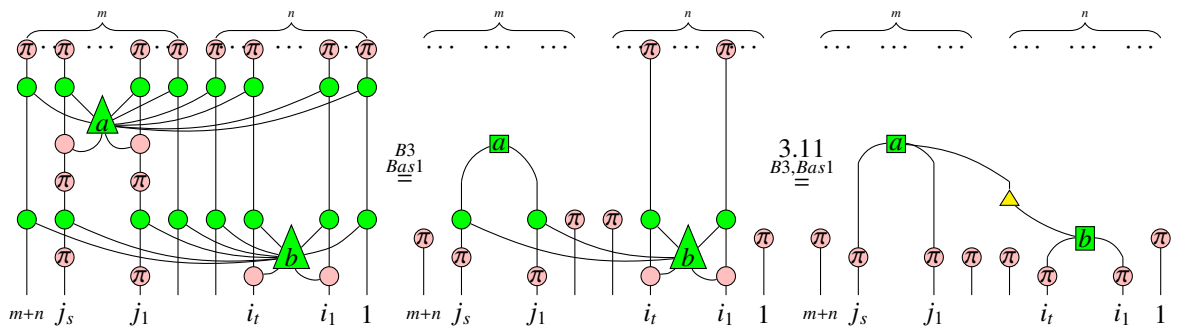


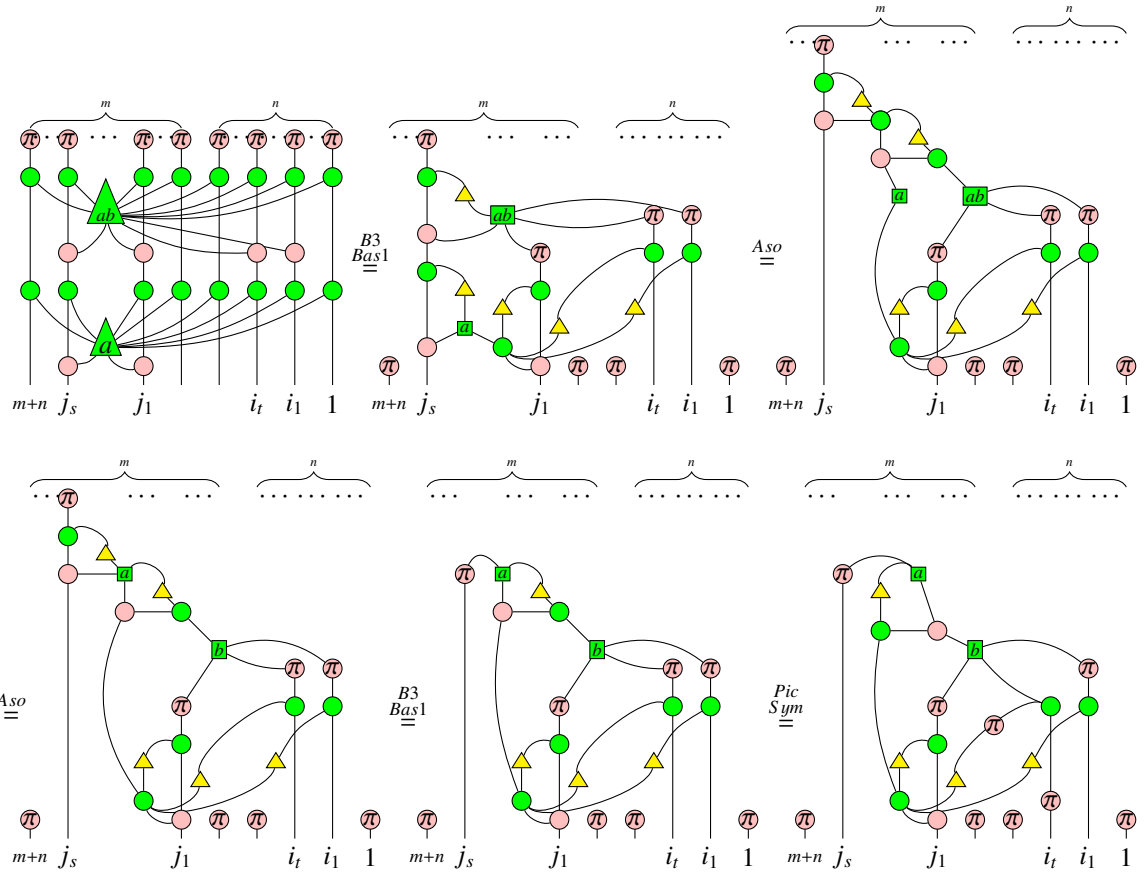
where the node  $ab$  is connected to  $j_1, \dots, j_s$  via pink nodes.

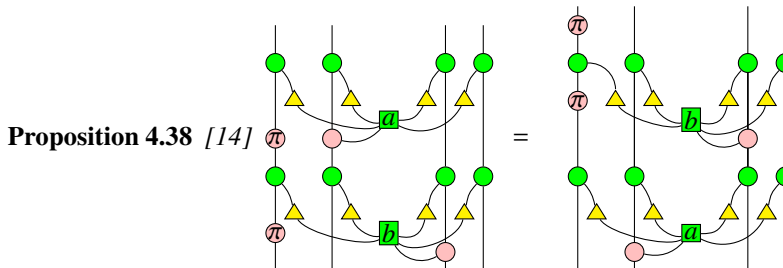
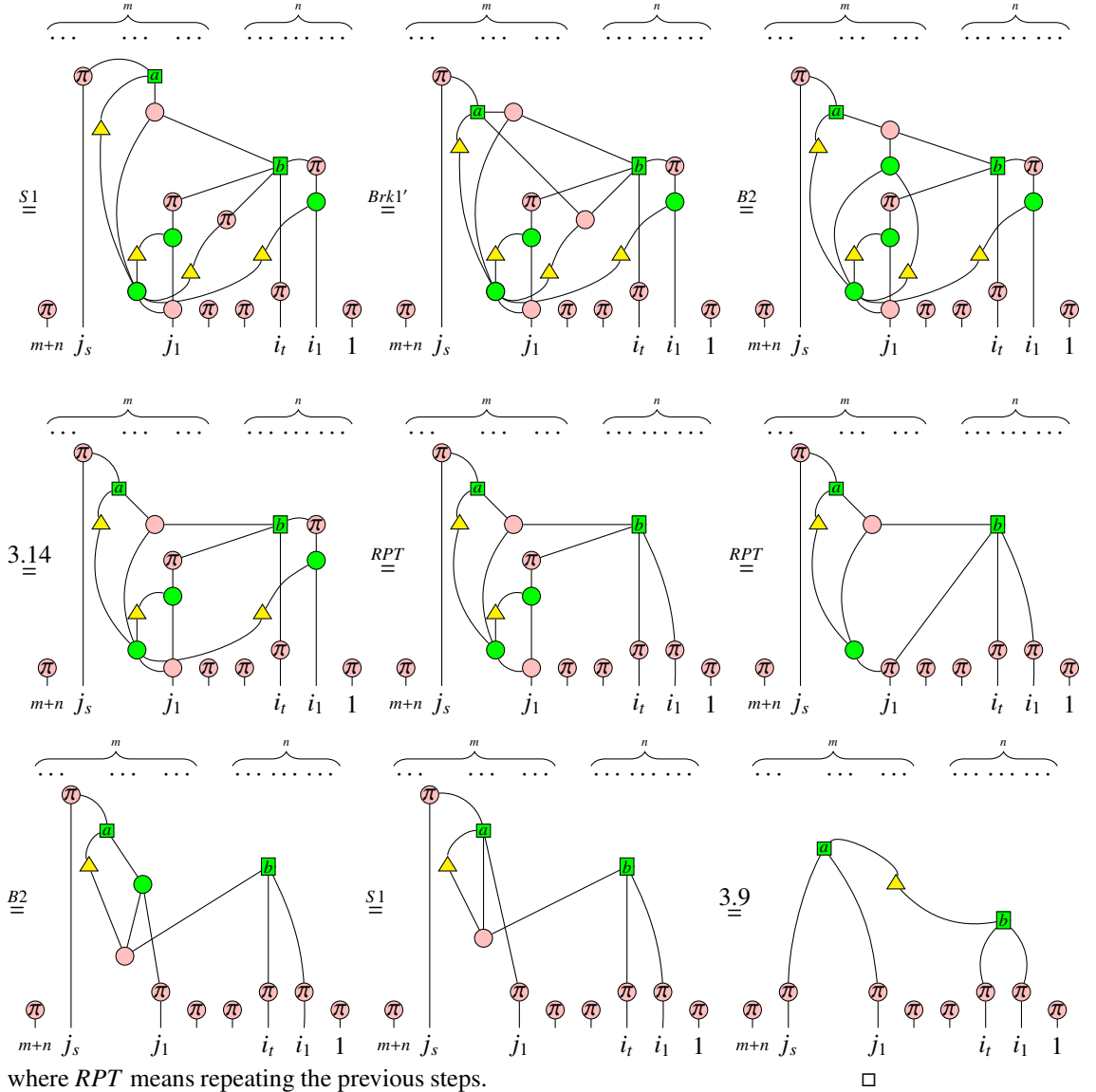
**Proposition 4.37** [14] Suppose the node  $a$  is connected to  $j_1, \dots, j_s$  via pink nodes, the node  $b$  is connected to  $i_1, \dots, i_t$  via pink nodes, pairs of red  $\pi$  nodes separated by green nodes connected to  $b$  are located on  $j_1, \dots, j_s$ . Furthermore,  $\emptyset \neq \{i_1, \dots, i_t\} \subseteq \{1, \dots, n\}$ ,  $\emptyset \neq \{j_1, \dots, j_s\} \subseteq \{n+1, \dots, n+m\}$ .



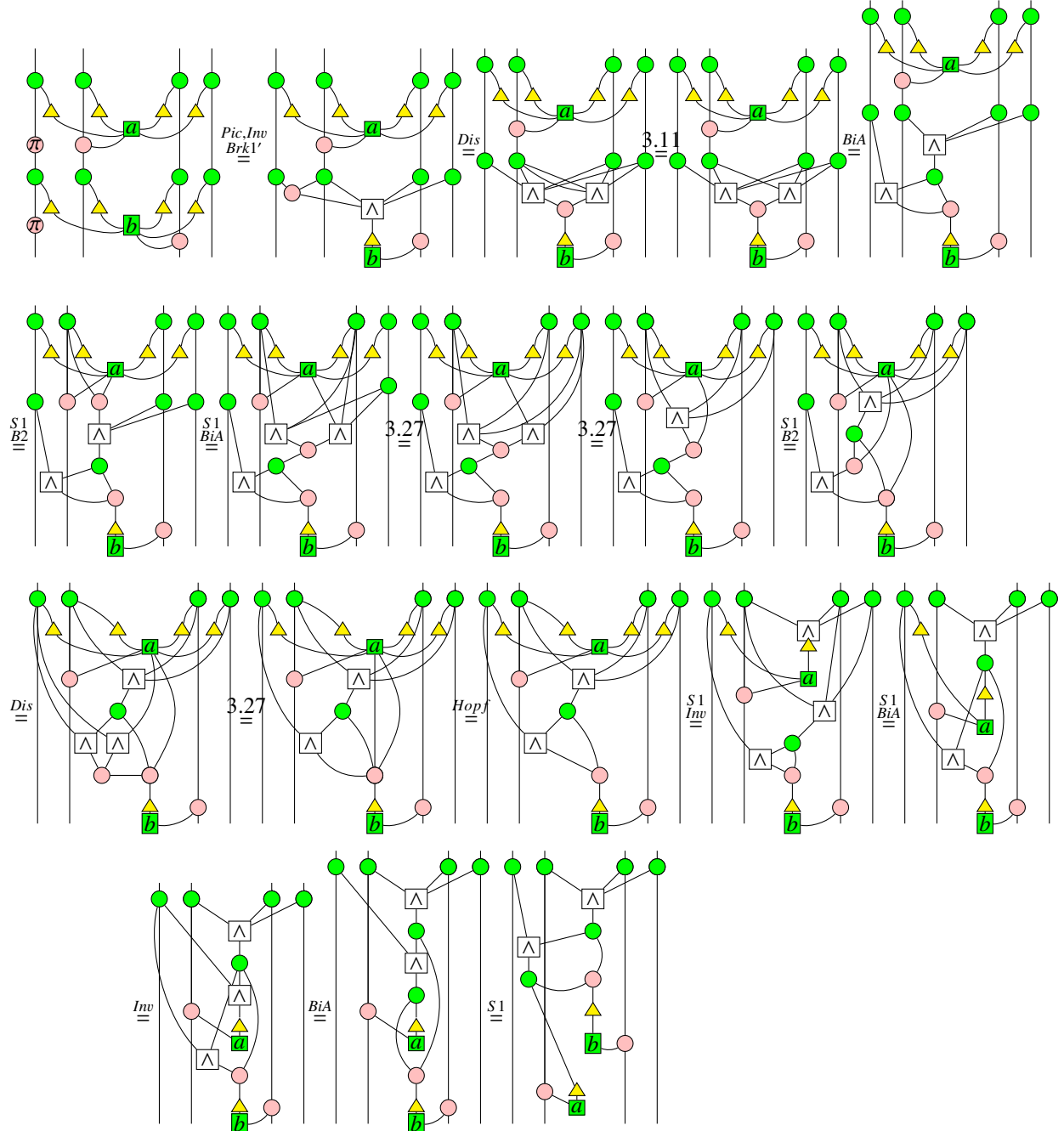
**Proof:** Assume that  $\{j_s\} \neq \emptyset$ . Then

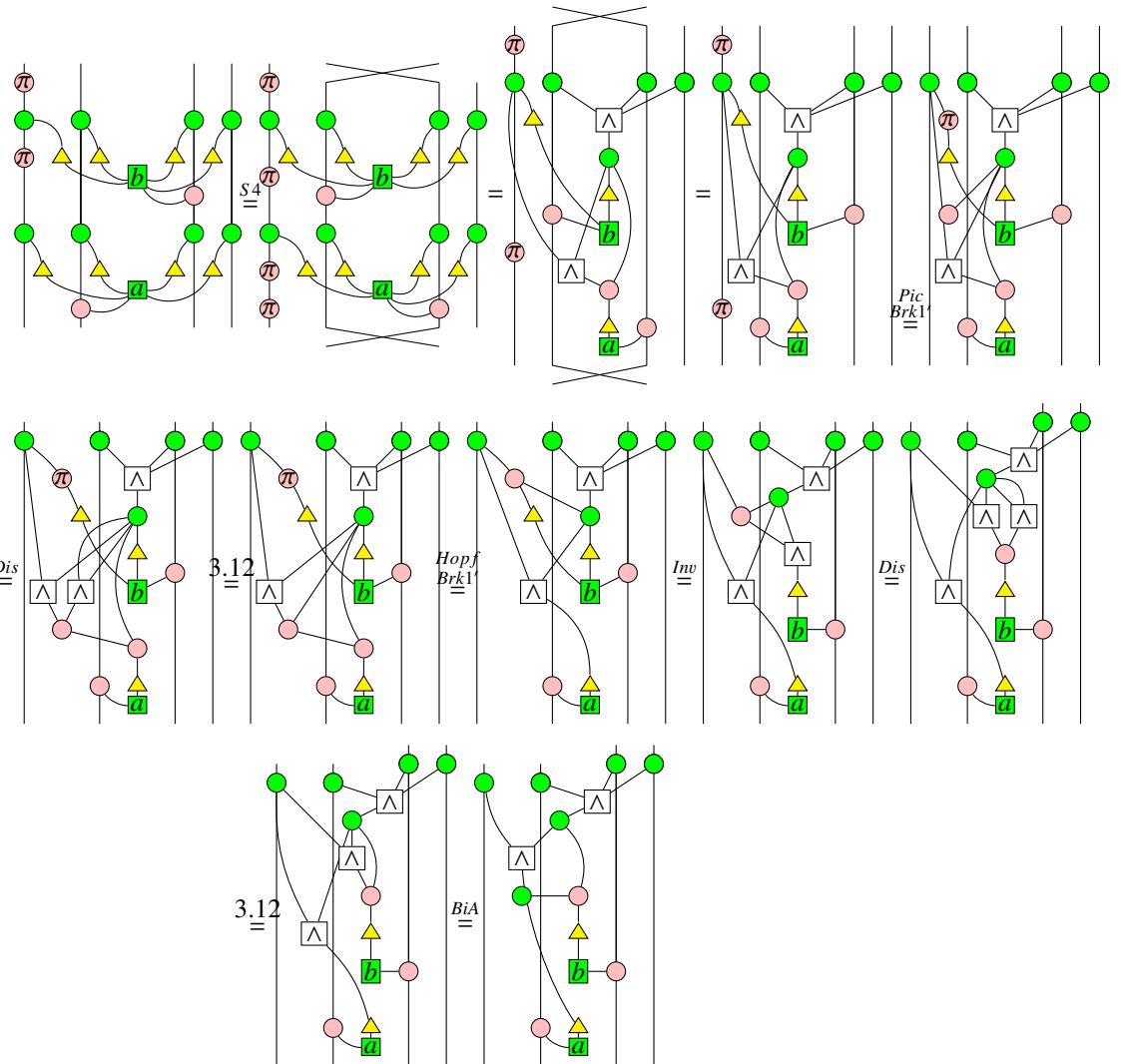






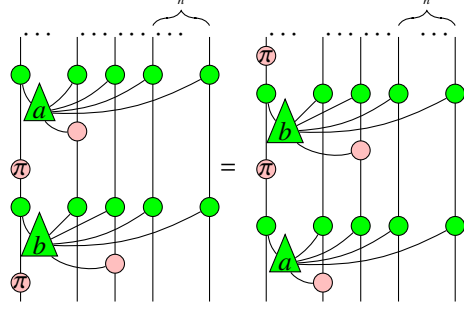
**Proof:**



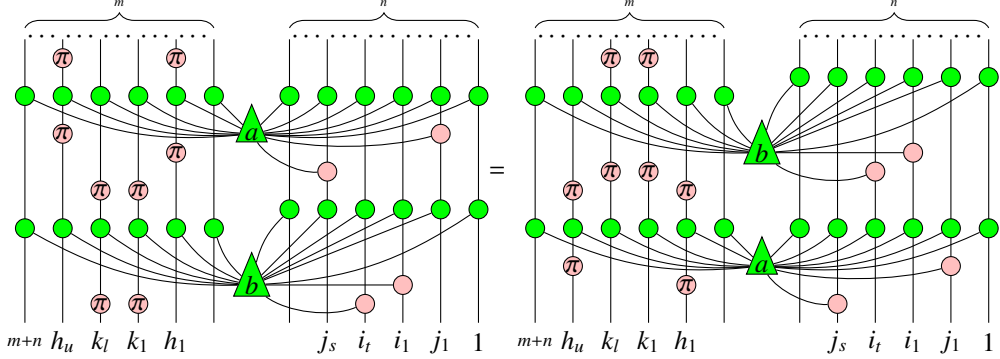


□

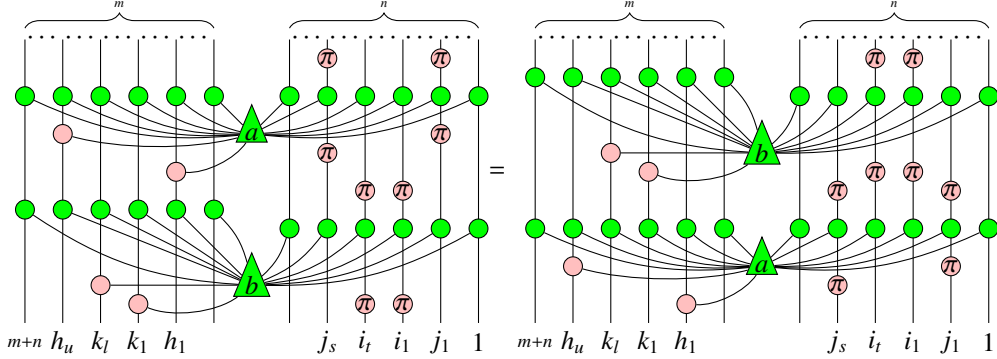
**Corollary 4.39** [14]



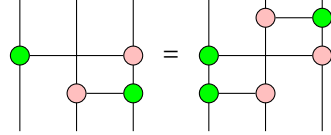
**Proposition 4.40** [14] Suppose the node  $a$  is connected to  $j_1, \dots, j_s$  via pink nodes, the node  $b$  is connected to  $i_1, \dots, i_t$  via pink nodes, pairs of red  $\pi$  nodes separated by green nodes connected to  $a$  are located on  $h_1, \dots, h_u$ , pairs of red  $\pi$  nodes separated by green nodes connected to  $b$  are located on  $k_1, \dots, k_l$ . Furthermore,  $\emptyset \neq \{i_1, \dots, i_t\} \subseteq \{1, \dots, n\}$ ,  $\emptyset \neq \{j_1, \dots, j_s\} \subseteq \{1, \dots, n\}$ ,  $\{h_1, \dots, h_u\} \subseteq \{n+1, \dots, n+m\}$ ,  $\{k_1, \dots, k_l\} \subseteq \{n+1, \dots, n+m\}$ . Then



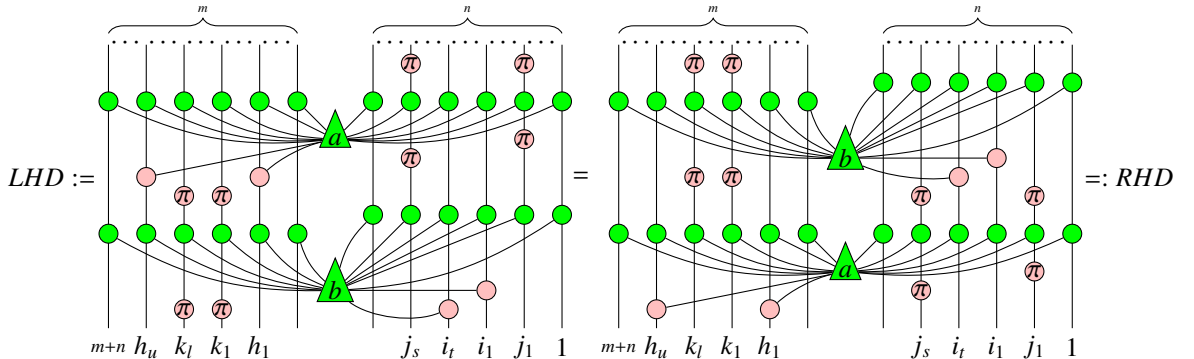
**Corollary 4.41** [14] Suppose the node  $a$  is connected to  $h_1, \dots, h_u$  via pink nodes, the node  $b$  is connected to  $k_1, \dots, k_l$  via pink nodes, pairs of red  $\pi$  nodes separated by green nodes connected to  $a$  are located on  $j_1, \dots, j_s$ , pairs of red  $\pi$  nodes separated by green nodes connected to  $b$  are located on  $i_1, \dots, i_t$ . Furthermore,  $\{i_1, \dots, i_t\} \subseteq \{1, \dots, n\}$ ,  $\{j_1, \dots, j_s\} \subseteq \{1, \dots, n\}$ ,  $\emptyset \neq \{h_1, \dots, h_u\} \subseteq \{n+1, \dots, n+m\}$ ,  $\emptyset \neq \{k_1, \dots, k_l\} \subseteq \{n+1, \dots, n+m\}$ . Then



**Lemma 4.42** [14]

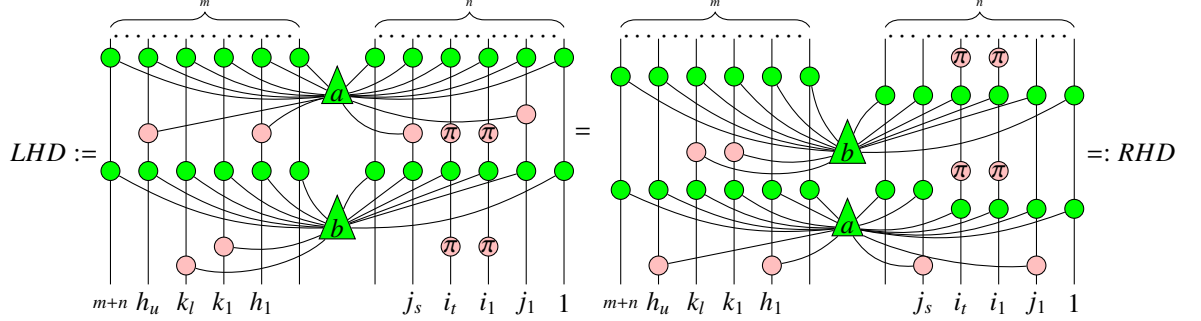


**Proposition 4.43** [14] Suppose the node  $a$  is connected to  $h_1, \dots, h_u$  via pink nodes, the node  $b$  is connected to  $i_1, \dots, i_t$  via pink nodes, pairs of red  $\pi$  nodes separated by green nodes connected to  $a$  are located on  $j_1, \dots, j_s$ , pairs of red  $\pi$  nodes separated by green nodes connected to  $b$  are located on  $k_1, \dots, k_l$ . Furthermore,  $\emptyset \neq \{i_1, \dots, i_t\} \subseteq \{1, \dots, n\}, \{j_1, \dots, j_s\} \subseteq \{1, \dots, n\}, \emptyset \neq \{h_1, \dots, h_u\} \subseteq \{n+1, \dots, n+m\}, \emptyset \neq \{k_1, \dots, k_l\} \subseteq \{n+1, \dots, n+m\}, \{h_1, \dots, h_u\} \neq \{k_1, \dots, k_l\}$ . Then

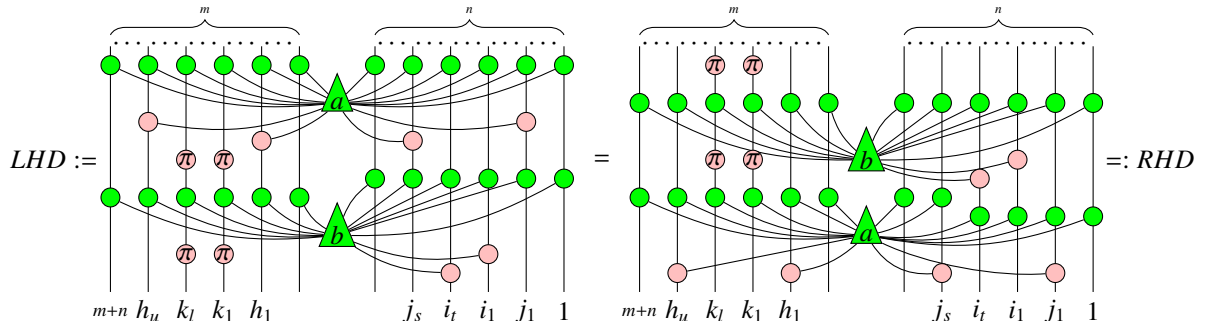


**Proposition 4.44** [14] Suppose the node  $a$  is connected to  $h_1, \dots, h_u$  on the left  $m$  wires via pink nodes, and is connected to  $j_1, \dots, j_s$  on the right  $n$  wires via pink nodes; the node  $b$  is connected to  $k_1, \dots, k_l$  via pink nodes, pairs of red  $\pi$  nodes separated by green nodes connected to  $b$  are located on  $i_1, \dots, i_t$ . Furthermore,  $\{i_1, \dots, i_t\} \subseteq \{1, \dots, n\}, \emptyset \neq \{j_1, \dots, j_s\} \subseteq \{1, \dots, n\}, \emptyset \neq \{h_1, \dots, h_u\} \subseteq \{n+1, \dots, n+m\}, \emptyset \neq$

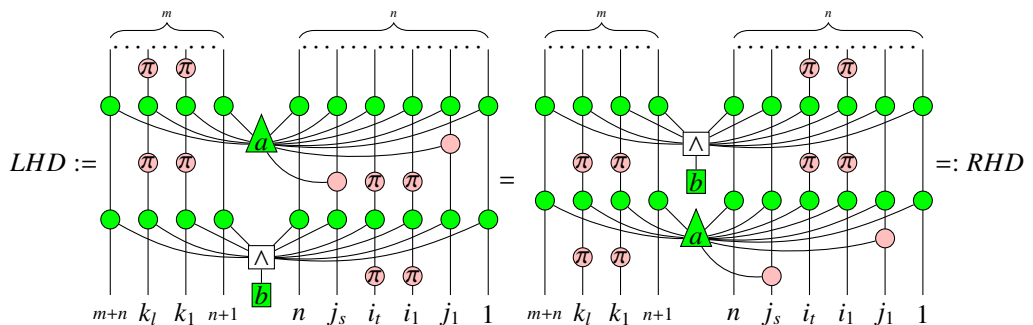
$\{k_1, \dots, k_l\} \subseteq \{n+1, \dots, n+m\}$ ,  $\{h_1, \dots, h_u\} \neq \{k_1, \dots, k_l\}$ . Then



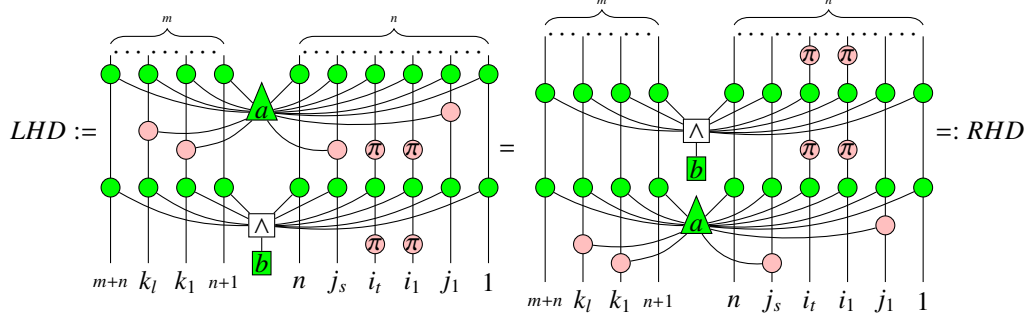
**Proposition 4.45** [14] Suppose the node  $a$  is connected to  $h_1, \dots, h_u$  on the left  $m$  wires via pink nodes, and is connected to  $j_1, \dots, j_s$  on the right  $n$  wires via pink nodes; the node  $b$  is connected to  $i_1, \dots, i_t$  via pink nodes, pairs of red  $\pi$  nodes separated by green nodes connected to  $b$  are located on  $k_1, \dots, k_l$ . Furthermore,  $\emptyset \neq \{i_1, \dots, i_t\} \subseteq \{1, \dots, n\}$ ,  $\emptyset \neq \{j_1, \dots, j_s\} \subseteq \{1, \dots, n\}$ ,  $\emptyset \neq \{h_1, \dots, h_u\} \subseteq \{n+1, \dots, n+m\}$ ,  $\{k_1, \dots, k_l\} \subseteq \{n+1, \dots, n+m\}$ ,  $\{h_1, \dots, h_u\} \neq \{k_1, \dots, k_l\}$ . Then



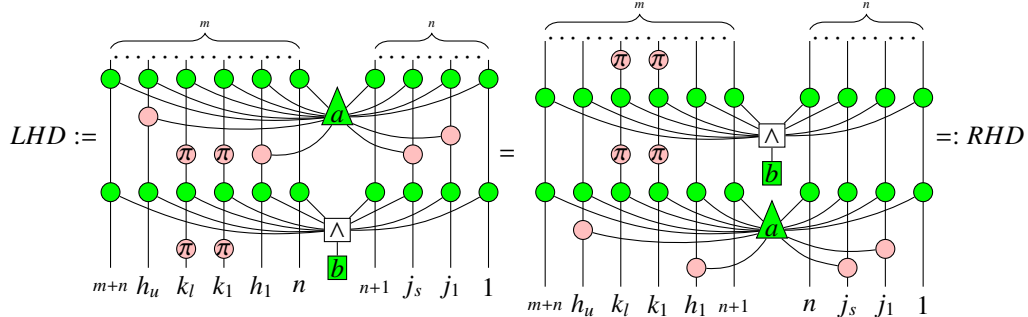
**Proposition 4.46** [14] Suppose the node  $a$  is connected to  $j_1, \dots, j_s$  on the right  $n$  wires via pink nodes, pairs of red  $\pi$  nodes separated by green nodes connected to  $a$  are located on  $k_1, \dots, k_l$ , pairs of red  $\pi$  nodes separated by green nodes connected to  $b$  are located on  $i_1, \dots, i_t$ . Furthermore,  $\{i_1, \dots, i_t\} \subseteq \{1, \dots, n\}$ ,  $\emptyset \neq \{j_1, \dots, j_s\} \subseteq \{1, \dots, n\}$ ,  $\emptyset \neq \{k_1, \dots, k_l\} \subseteq \{n+1, \dots, n+m\}$ . Then



**Proposition 4.47** [14] Suppose the node  $a$  is connected to  $j_1, \dots, j_s$  on the right  $n$  wires via pink nodes, and connected to  $k_1, \dots, k_l$  on the left  $m$  wires via pink nodes; pairs of red  $\pi$  nodes separated by green nodes connected to  $b$  are located on  $i_1, \dots, i_t$ . Furthermore,  $\emptyset \neq \{i_1, \dots, i_t\} \subseteq \{1, \dots, n\}$ ,  $\emptyset \neq \{j_1, \dots, j_s\} \subseteq \{1, \dots, n\}$ ,  $\emptyset \neq \{k_1, \dots, k_l\} \subseteq \{n+1, \dots, n+m\}$ . Then



**Corollary 4.48** [14] Suppose the node  $a$  is connected to  $j_1, \dots, j_s$  on the right  $n$  wires via pink nodes, and connected to  $h_1, \dots, h_u$  on the left  $m$  wires via pink nodes; pairs of red  $\pi$  nodes separated by green nodes connected to  $b$  are located on  $k_1, \dots, k_l$ . Furthermore,  $\emptyset \neq \{j_1, \dots, j_s\} \subseteq \{1, \dots, n\}$ ,  $\emptyset \neq \{k_1, \dots, k_l\} \subseteq \{n+1, \dots, n+m\}$ ,  $\emptyset \neq \{h_1, \dots, h_u\} \subseteq \{n+1, \dots, n+m\}$ . Then



**Proposition 4.49** [14] Suppose the node  $a$  is connected to  $j_1, \dots, j_s$  on the right  $n$  wires via pink nodes, pairs of red  $\pi$  nodes separated by green nodes connected to  $b$  are located on  $i_1, \dots, i_t$ . Furthermore,  $\emptyset \neq \{i_1, \dots, i_t\} \subseteq \{1, \dots, n\}$ ,  $\emptyset \neq \{j_1, \dots, j_s\} \subseteq$

$\{1, \dots, n\}, \{i_1, \dots, i_t\} \neq \{j_1, \dots, j_s\}$ . Then

$$\begin{array}{ccc}
 \text{LHD} := & \text{Diagram showing a network of wires connecting nodes } a \text{ and } b \text{ through various nodes and gates.} & =: \text{RHD}
 \end{array}$$

**Corollary 4.50** [14] Suppose the node  $a$  is connected to  $j_1, \dots, j_s$  on the left  $m$  wires via pink nodes, pairs of red  $\pi$  nodes separated by green nodes connected to  $b$  are located on  $i_1, \dots, i_t$ . Furthermore,  $\emptyset \neq \{i_1, \dots, i_t\} \subseteq \{1+n, \dots, m+n\}$ ,  $\emptyset \neq \{j_1, \dots, j_s\} \subseteq \{1+n, \dots, m+n\}$ ,  $\{i_1, \dots, i_t\} \neq \{j_1, \dots, j_s\}$ . Then

$$\begin{array}{ccc}
 \text{Diagram showing a network of wires connecting nodes } a \text{ and } b \text{ through various nodes and gates.} & = & \text{Diagram showing a network of wires connecting nodes } a \text{ and } b \text{ through various nodes and gates.}
 \end{array}$$

## 5 Completeness of ZX-calculus over $\mathcal{R}$ via elementary transformations

In this section, we prove the main theorem totally following [14]. For simplicity, we omit the corresponding details in [14] if they still hold in this paper.

**Theorem 5.1** The ZX-calculus over an arbitrary ring  $\mathcal{R}$  is complete with respect to the rules in Figure 1 and Figure 2.

## 5.1 Normal form

Suppose that  $a_j \in \mathcal{R}, 0 \leq j_1 < \dots < j_s \leq m-1, 1 \leq s \leq m$ . Then the following diagram



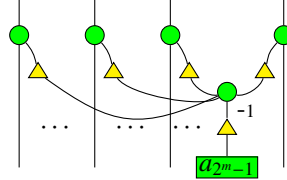
where  $a_j$  connects to  $j_1, \dots, j_s$  via red dots, represents the  $2^m \times 2^m$  row-addition elementary matrix:

$$A_j = \begin{pmatrix} 1 & \cdots & 0 & \cdots & 0 \\ \vdots & \ddots & & & \vdots \\ 0 & \cdots & 1 & \cdots & a_j \\ \vdots & & & \ddots & \vdots \\ 0 & \cdots & 0 & \cdots & 1 \end{pmatrix} r_j$$

$$r_0 \quad r_j \quad r_{2^m-1}$$

where  $a_j$  lies in the  $r_j$  row,  $j = 2^m - 1 - (2^{j_1} + \dots + 2^{j_s})$ .

Moreover, let  $a_{2^m-1} \in \mathcal{R}$ , then the following diagram



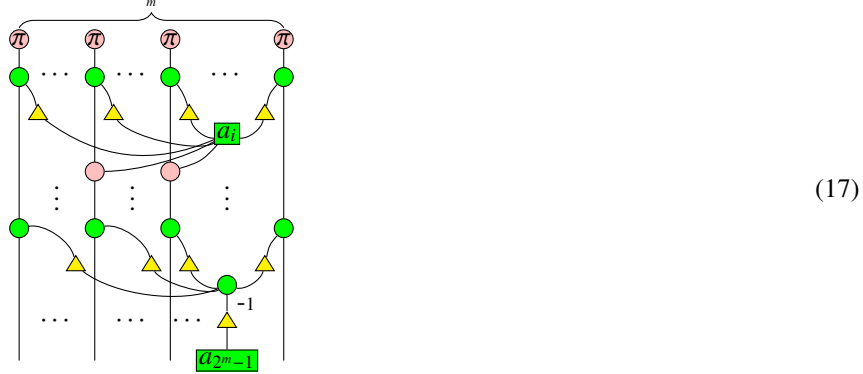
represents the row-multiplication matrix:

$$M = \begin{pmatrix} 1 & \cdots & 0 & \cdots & 0 \\ \vdots & \ddots & & & \vdots \\ 0 & \cdots & 1 & \cdots & 0 \\ \vdots & & & \ddots & \vdots \\ 0 & \cdots & 0 & \cdots & a_{2^m-1} \end{pmatrix} r_k$$

$$r_0 \quad r_k \quad r_{2^m-1}$$

Any vector  $(a_0, a_1, \dots, a_{2^m-1})^T$  with  $a_i \in \mathcal{R}, m \geq 1$  can be uniquely represented by

the following normal form:



where for those diagrams which represent row additions,  $a_i$  connects to wires with pink nodes depending on  $i$ , and all possible connections are included in the normal form. Actually, one can check that there are  $\binom{m}{1} + \binom{m}{2} + \dots + \binom{m}{m} = 2^m - 1$  row additions in the normal form. By Proposition 4.25, all the row addition diagrams are commutative with each other.

In the case of  $m = 0$ , for any element  $a \in \mathcal{R}$ , its normal form is defined as



where

$$\llbracket \begin{array}{c} \pi \\ a \end{array} \rrbracket = a$$

By the map-state duality as given in (??), we obtain the universality of ZX-calculus over  $\mathcal{R}$ : any  $2^m \times 2^n$  matrix  $A$  with  $m, n \geq 0$  can be represented by a ZX diagram.

## 5.2 Proof of completeness

Completeness means for any two diagrams  $D_1$  and  $D_2$  of ZX-calculus over  $\mathcal{R}$ , if  $\llbracket D_1 \rrbracket = \llbracket D_2 \rrbracket$ , then  $D_1 = D_2$  can be derived from the ZX rules. As shown in [14], to prove completeness we need to prove the following statements:

1. the juxtaposition of any two diagrams in normal form can be rewritten into a normal form.
2. a self-plugging on a diagram in normal form can be rewritten into a normal form.
3. all generators bended in state diagrams or already being state diagrams can be rewritten into normal forms.

### 5.2.1 Rewrite the tensor product of two normal forms into a normal form

It has been simply shown in [14] that the tensor product of two scalar diagrams can be rewritten into a normal form as follows:

$$\begin{array}{c} \text{Diagram 1} \\ \text{Diagram 2} \end{array} \xrightarrow{B3} \begin{array}{c} \text{Diagram 3} \\ \text{Diagram 4} \end{array} \xrightarrow{S1} \begin{array}{c} \text{Diagram 5} \\ \text{Diagram 6} \end{array}$$

Given the following two norm forms such that

$$\begin{array}{c} \text{Diagram 7} \\ \text{Diagram 8} \end{array} = \begin{pmatrix} a_0 \\ a_1 \\ \vdots \\ a_{2^m-2} \\ a_{2^m-1} \end{pmatrix} \quad (18)$$

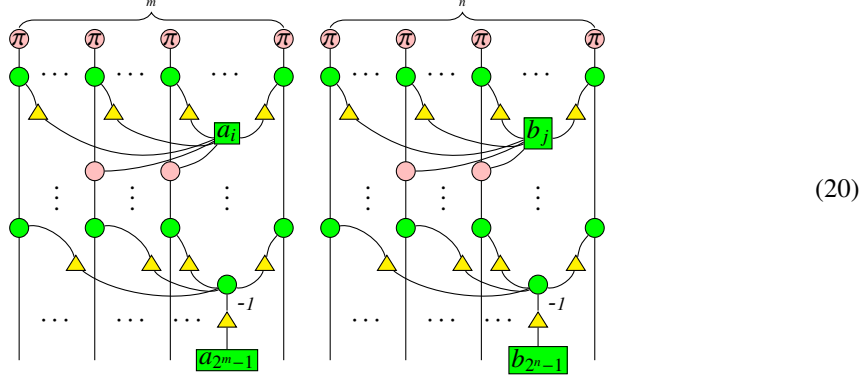
and

$$\begin{array}{c} \text{Diagram 9} \\ \text{Diagram 10} \end{array} = \begin{pmatrix} b_0 \\ b_1 \\ \vdots \\ b_{2^n-2} \\ b_{2^n-1} \end{pmatrix} \quad (19)$$

where  $m, n$  are positive integers,  $a_i, b_j \in \mathcal{R}$ , we have

**Proposition 5.2** *The following tensor product of two normal forms can be rewritten*

into a single normal form:



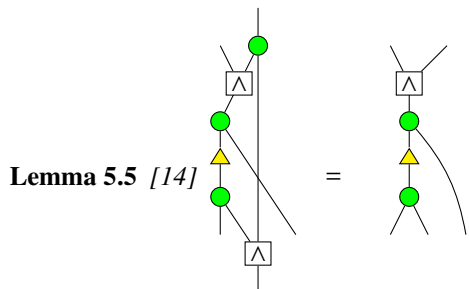
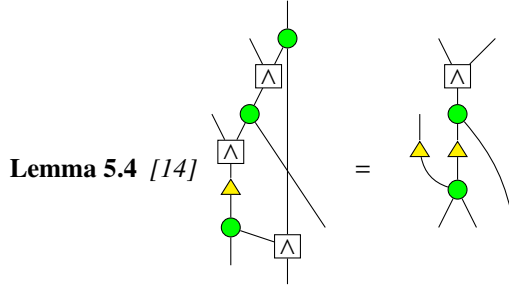
The proof of this proposition is the same as that of [14].

### 5.2.2 Self-plugging on a normal form

In this subsection, we prove the following result:

**Theorem 5.3** *A self-plugged normal form can be rewritten into a normal form.*

The proof given in [14] still holds here. In the following we show again the properties used for this proof, where only one proposition need a new proof which works for the ring case.



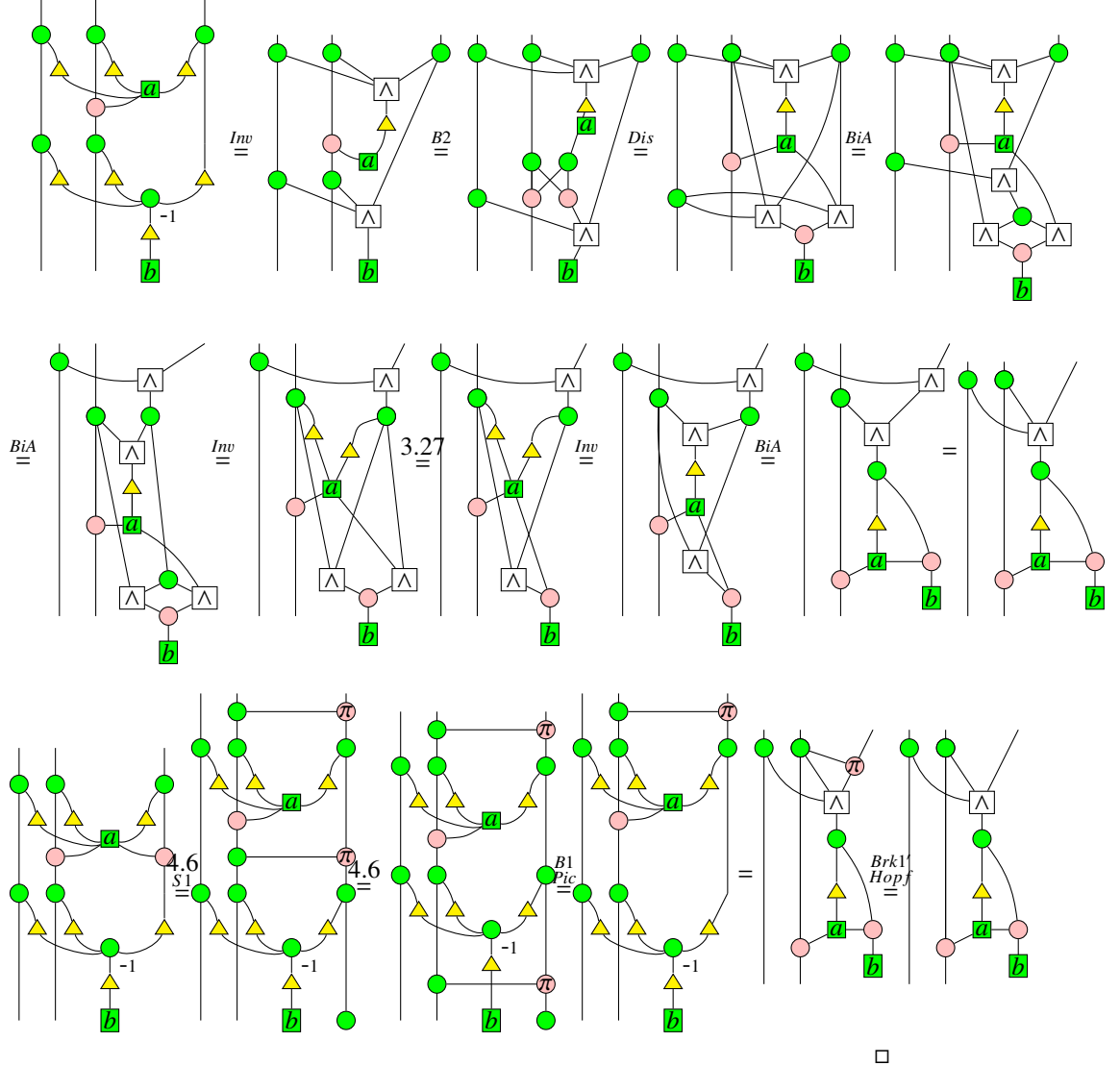
**Proposition 5.6** [14]

(21)

**Corollary 5.7** [14]

**Proposition 5.8** [14]

**Proof:**



**Corollary 5.9** [14] Suppose  $a$  is connected to the  $i$ -th line via a pink node ( $i > 1$ ).

Then

(22)

where on the left side of (22) the node  $a$  is connected to the  $i$ -th line and the 1st line via two pink nodes.

**Proposition 5.10** [14] Suppose  $a$  is connected to the  $i_1, \dots, i_s$  via pink nodes ( $i_1 > 1$ ). Then one more connection can be added on the right most line:

(23)

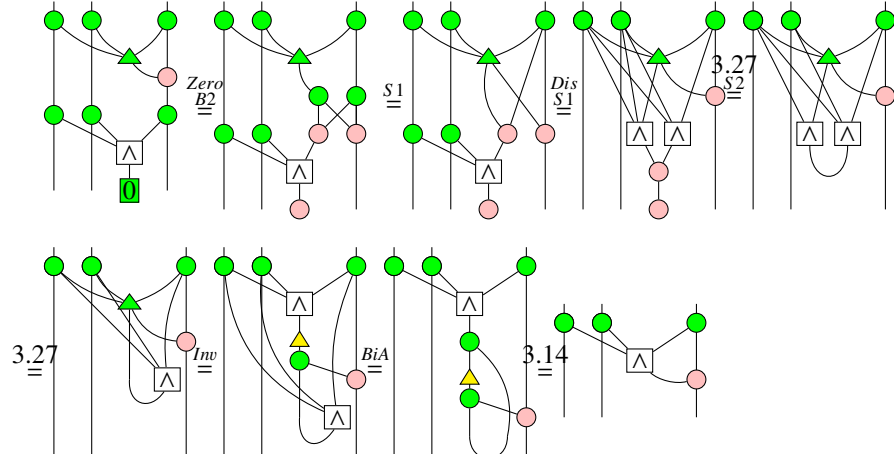
### 5.2.3 Rewriting generators into normal form

In this section, we prove that all the generators bended in state diagrams or already being state diagrams can be rewritten into normal forms.

We only need to rewrite the generators  $R_X^{(n,m)}$  and  $P$  in Table 1 into a normal form, since the other generators have been rewritten into normal form in [14].

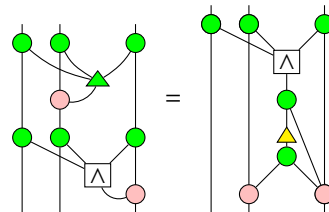
#### Lemma 5.11

**Proof:**

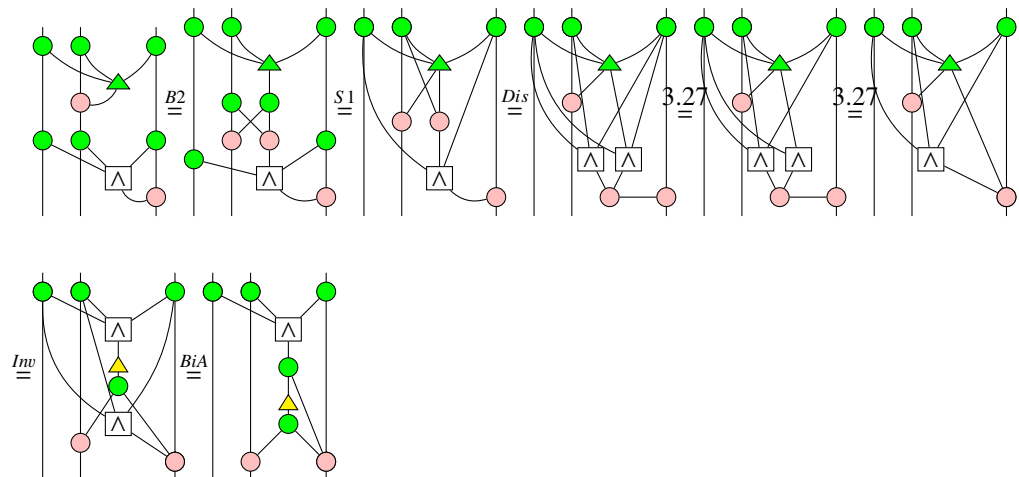


□

**Lemma 5.12**

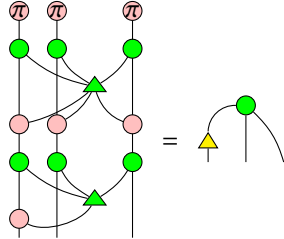


**Proof:**

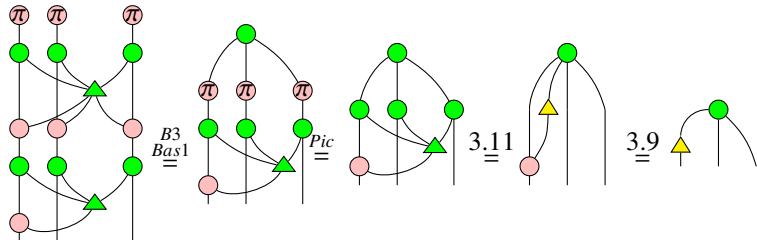


□

**Lemma 5.13**

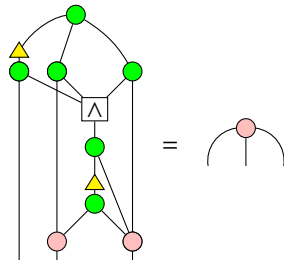


**Proof:**

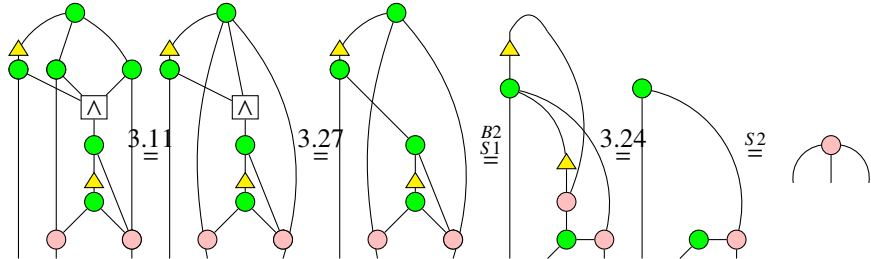


□

**Lemma 5.14**

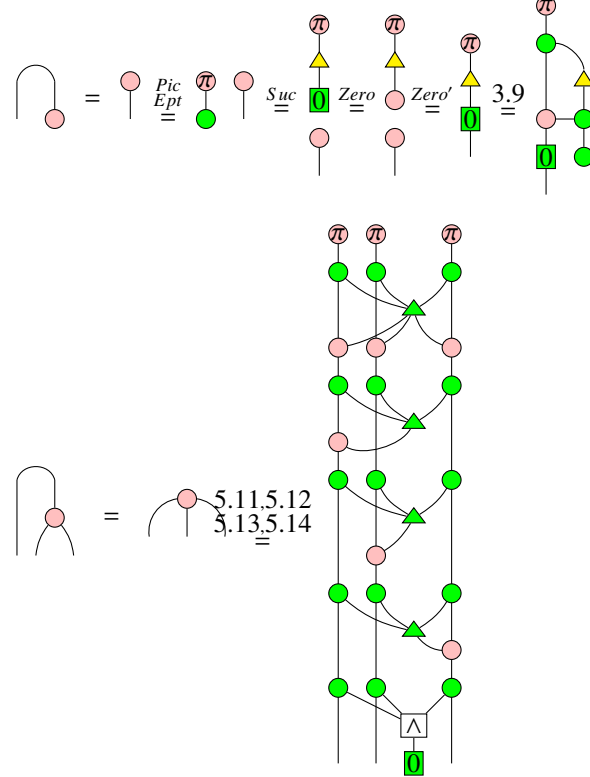


**Proof:**

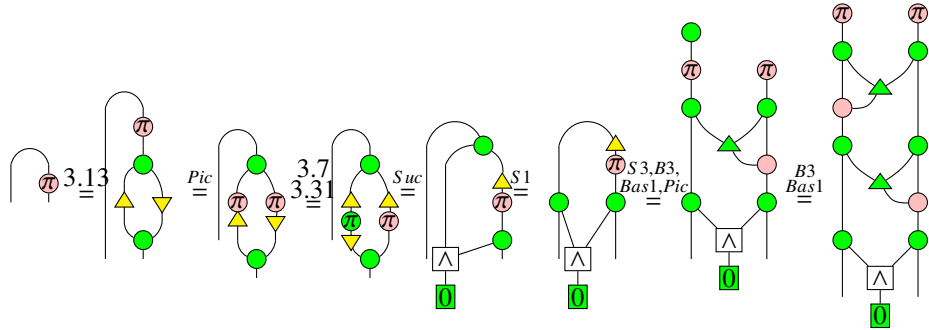


□

1. For  $R_X^{(n,m)}$ , it is reduced to the following two cases:



2. For the generator  $P$ , we have



#### 5.2.4 Rewriting scalars into normal form

Given an arbitrary scalar diagram over a ring  $\mathcal{R}$ , due to Lemma 3.2, it can be seen as a state diagram on top plugged with cups or from the bottom. Such a state diagram has been shown in the previous subsection that it can be rewritten into a normal form. In addition, a normal form plugged with can be bended up, so at the end any

scalar diagram is a non-scalar normal form with outputs connected only by cups. Since normal form with more than 2 outputs plugged with cups can be reduced to a normal form with outputs as proved in Theorem 5.3, we just need to show that a normal form with exactly 2 outputs plugged with a cup can be written into a scalar normal form  $\text{a}^\text{t}$ , which has also been obtained in Theorem 5.3.

## 6 ZX-calculus over commutative semirings

Given an arbitrary commutative semiring  $\mathcal{S}$ , it is clear that one could not have a Hadamard node or an inverse of the triangle node any more, due to a short of negative elements. Bearing this in mind, we give the generators of ZX-calculus over  $\mathcal{S}$  in the following table.

$R_{Z,a}^{(n,m)} : n \rightarrow m$	$R_X^{(n,m)} : n \rightarrow m$
$T : 1 \rightarrow 1$	$\sigma : 2 \rightarrow 2$
$\mathbb{I} : 1 \rightarrow 1$	$P : 1 \rightarrow 1$
$C_a : 0 \rightarrow 2$	$C_u : 2 \rightarrow 0$

Table 2: Generators of ZX-calculus, where  $m, n \in \mathbb{N}$ ,  $a \in \mathcal{S}$ , and  $e$  represents an empty diagram.

There is a standard interpretation  $\llbracket \cdot \rrbracket$  for the ZX diagrams over  $\mathcal{S}$ :

$$\llbracket \text{a} \rrbracket = |0\rangle^{\otimes m} \langle 0|^{\otimes n} + a |1\rangle^{\otimes m} \langle 1|^{\otimes n},$$

$$\left[ \begin{array}{c} \text{Diagram of a red spider with } n \text{ inputs and } m \text{ outputs} \end{array} \right] = \sum_{\substack{i_1, \dots, i_m, j_1, \dots, j_n \in \{0,1\} \\ i_1 + \dots + i_m \equiv j_1 + \dots + j_n \pmod{2}}} |i_1, \dots, i_m\rangle \langle j_1, \dots, j_n|,$$

$$\left[ \begin{array}{c} \text{Diagram with a yellow triangle} \end{array} \right] = \begin{pmatrix} 1 & 1 \\ 0 & 1 \end{pmatrix}, \quad \left[ \begin{array}{c} \cdot & \cdot & \cdot \\ \vdots & \ddots & \vdots \\ \cdot & \cdot & \cdot \end{array} \right] = 1, \quad \left[ \begin{array}{c} \cdot \\ \vdots \\ \cdot \end{array} \right] = \begin{pmatrix} 1 & 0 \\ 0 & 1 \end{pmatrix}, \quad \left[ \begin{array}{c} \text{Diagram with a red circle} \end{array} \right] = \begin{pmatrix} 0 & 1 \\ 1 & 0 \end{pmatrix},$$

$$\left[ \begin{array}{c} \text{Diagram with a red cross} \end{array} \right] = \begin{pmatrix} 1 & 0 & 0 & 0 \\ 0 & 0 & 1 & 0 \\ 0 & 1 & 0 & 0 \\ 0 & 0 & 0 & 1 \end{pmatrix}, \quad \left[ \begin{array}{c} \text{Diagram with a red curve} \end{array} \right] = \begin{pmatrix} 1 \\ 0 \\ 0 \\ 1 \end{pmatrix}, \quad \left[ \begin{array}{c} \text{Diagram with a red wavy line} \end{array} \right] = (1 \ 0 \ 0 \ 1),$$

$$[D_1 \otimes D_2] = [D_1] \otimes [D_2], \quad [D_1 \circ D_2] = [D_1] \circ [D_2],$$

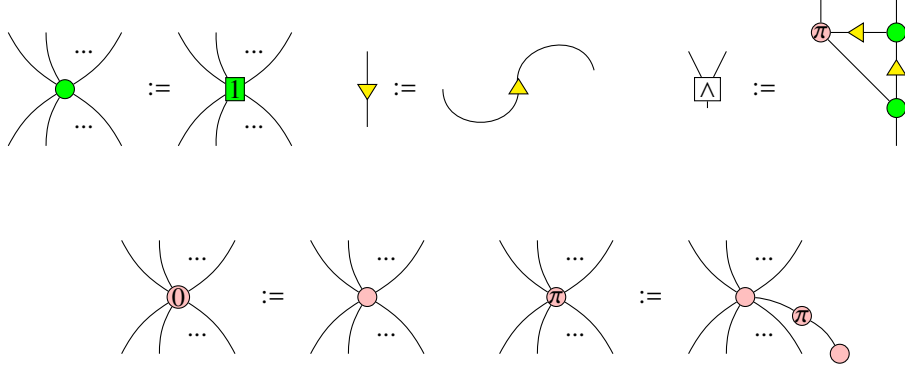
where

$$a \in \mathcal{S}, \quad |0\rangle = \begin{pmatrix} 1 \\ 0 \end{pmatrix}, \quad \langle 0| = (1 \ 0), \quad |1\rangle = \begin{pmatrix} 0 \\ 1 \end{pmatrix}, \quad \langle 1| = (0 \ 1), \quad \begin{array}{c} \cdot & \cdot & \cdot \\ \vdots & \ddots & \vdots \\ \cdot & \cdot & \cdot \end{array}$$

denotes the empty diagram.

**Remark 6.1** If  $\mathcal{S} = \mathbb{C}$ , then the interpretation of the red spider we defined here is just the normal red spider [3] written in terms of computational basis with all the coefficients being 1. To see this, one just need to notice that the red spider can be generated by the monoid pair (and its flipped version)   corresponding to matrices  $\begin{pmatrix} 1 & 0 & 0 & 1 \\ 0 & 1 & 1 & 0 \end{pmatrix}$  and  $\begin{pmatrix} 1 \\ 0 \end{pmatrix}$  respectively, which means the red spider defined in this way is the same as the normal red spider (see e.g. [3]) up to a scalar depending on the number of inputs and outputs of the spider.

For simplicity, we make the following conventions:



Now we give rules for ZX-calculus over an arbitrary commutative semiring  $\mathcal{S}$ .

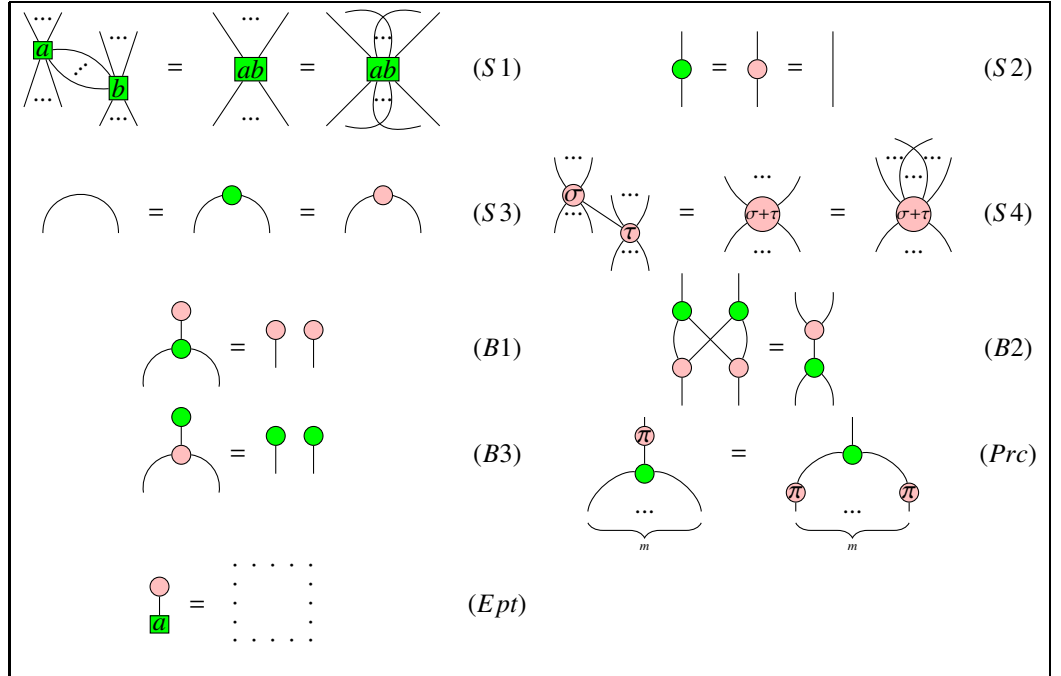
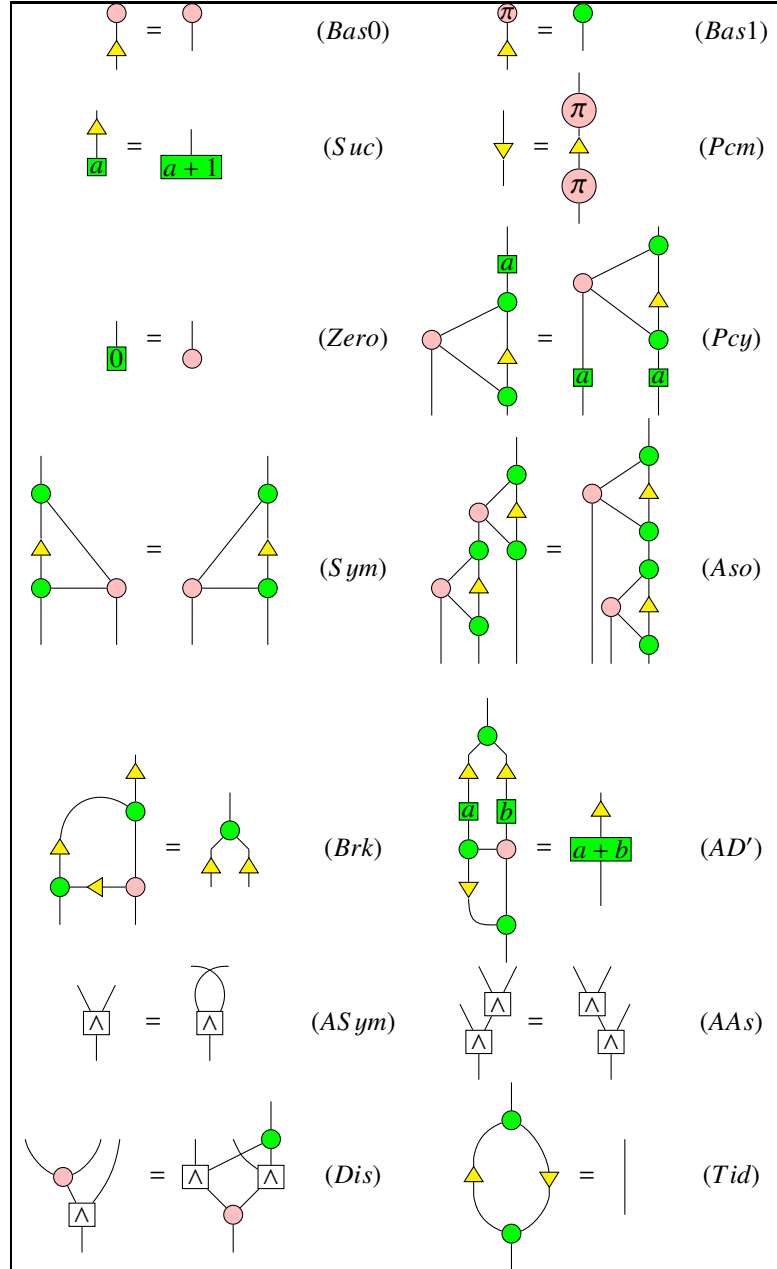


Figure 3: ZX rules I, over an arbitrary commutative semiring  $\mathcal{S}$ ,  $m \geq 0$ ,  $a, b \in \mathcal{S}$ ,  $\sigma, \tau \in \{0, \pi\}$ ,  $+$  is a modulo  $2\pi$  addition in (S4). The upside-down flipped versions of the rules are assumed to hold as well.



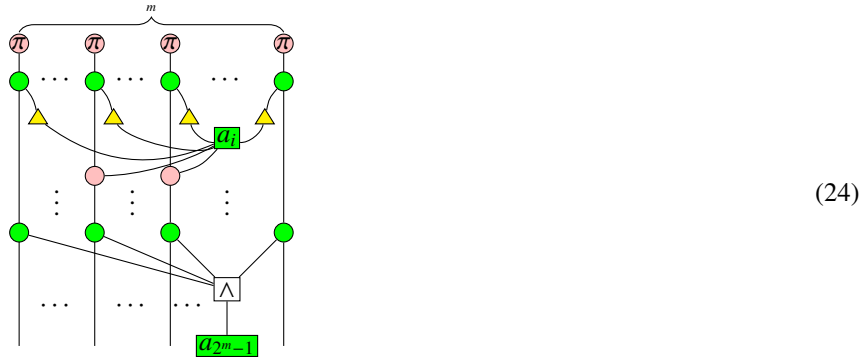
Due to the associative rule (AAs) for the AND gate, the following notation is well defined:

$$\cdots \begin{array}{c} \diagup \\ \square \end{array} \cdots := \begin{array}{c} \diagup \quad \diagdown \\ \square \quad \square \end{array} \cdots$$

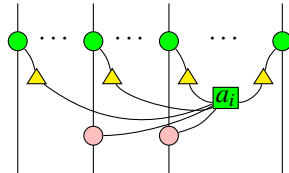
It is a routine check that these rules are sound in the sense that they still hold under the standard interpretation  $\llbracket \cdot \rrbracket$ .

## 7 Normal form, universality and completeness over commutative semirings

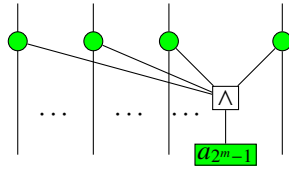
Given an arbitrary commutative semiring  $\mathcal{S}$ , any vector  $(a_0, a_1, \dots, a_{2^m-1})^T$  with  $a_i \in \mathcal{S}$  can be uniquely represented by the following normal form:



where  $a_i$  connects to wires by red nodes depending on  $i$ , and all possible connections are included in the normal form. We point out that the diagram



represents a matrix row addition from the bottom row, and the diagram



represents a matrix row multiplication on the bottom row multiplied by  $a_{2^m-1}$ . Note that

$$\left[ \begin{array}{c} \pi \\ \dots \\ \pi \end{array} \right] = \begin{pmatrix} 0 \\ \vdots \\ 1 \end{pmatrix},$$

the normal form (24) is actually obtained via the following processes:

$$\begin{pmatrix} 0 \\ 0 \\ \vdots \\ 1 \end{pmatrix} \xrightarrow[\text{row addition}]{\text{row}} \begin{pmatrix} a_0 \\ 0 \\ \vdots \\ 1 \end{pmatrix} \xrightarrow[\text{row addition}]{\text{row}} \begin{pmatrix} a_0 \\ a_1 \\ \vdots \\ a_{2^m-1} \\ 1 \end{pmatrix} \xrightarrow[\text{multiplication}]{\text{row}} \begin{pmatrix} a_0 \\ a_1 \\ \vdots \\ a_{2^m-2} \\ a_{2^m-1} \end{pmatrix}$$

By the map-state duality, we obtain the universality of ZX-calculus over an arbitrary commutative semiring.

For proof of completeness, we need to prove the following statements:

- the juxtaposition of any two diagrams in normal form can be rewritten into a normal form.
- a self-plugging on a diagram in normal form can be rewritten into a normal form.
- all generators can be rewritten into normal forms.

The method of proof of completeness for ZX-calculus over an arbitrary commutative semiring is the same as we showed for ZX-calculus over commutative rings, we will give the details in a later version.

## 8 Conclusion and further work

In this paper, we generalise ZX-calculus over the field of complex numbers to ZX-calculus over arbitrary commutative rings and semirings, by providing the corresponding generators and rewriting rules. Furthermore, we follow the method in [14] to prove that ZX-calculus over an arbitrary commutative ring is complete for matrices over the same ring.

The next apparent thing to do is to fill the details of the proof of completeness for ZX-calculus over an arbitrary commutative semiring. Another interesting is to do elementary number theory in the framework of ZX-calculus over the ring of integers. Furthermore, since we have presented all the elementary matrices in ZX form in [15], one could try to do linear algebra in an arbitrary commutative ring with string diagrams. Finally, we could also generalise ZX-calculus over rings or semirings to higher dimensional cases.

## Acknowledgements

This work is supported by AFOSR grant FA2386-18-1-4028. The author would like to thank Aleks Kissinger for useful discussions.

## References

- [1] Miriam Backens, Simon Perdrix & Quanlong Wang (2017): *A Simplified Stabilizer ZX-calculus*. *Electronic Proceedings in Theoretical Computer Science* 236, pp. 1–20, doi:10.4204/eptcs.236.1. Available at <http://dx.doi.org/10.4204/EPTCS.236.1>.
- [2] John C. Baez, Brandon Coya & Franciscus Rebro (2017): *Props in Network Theory*. arXiv:1707.08321.
- [3] Bob Coecke & Ross Duncan (2011): *Interacting quantum observables: categorical algebra and diagrammatics*. *New Journal of Physics* 13(4), p. 043016. Available at <http://stacks.iop.org/1367-2630/13/i=4/a=043016>. doi:10.1088/1367-2630/13/4/043016.
- [4] Bob Coecke, Ross Duncan, Aleks Kissinger & Quanlong Wang (2012): *Strong Complementarity and Non-locality in Categorical Quantum Mechanics*. In: *Proceedings of the 2012 27th Annual IEEE/ACM Symposium on Logic in Computer Science*, LICS ’12, IEEE Computer Society, pp. 245–254. doi:10.1109/LICS.2012.35.
- [5] Bob Coecke & Aleks Kissinger (2017): *Picturing quantum processes*. Cambridge University Press.
- [6] Bob Coecke & Quanlong Wang (2018): *ZX-rules for 2-qubit Clifford+T Quantum Circuits*. In: *Proceedings of the 10th International Conference, Reversible Computation 2018*, LNCS, pp. 144–161. doi:10.1007/978-3-319-99498-7\_10.
- [7] Amar Hadzihasanovic (2015): *A Diagrammatic Axiomatisation for Qubit Entanglement*. In: *2015 30th Annual ACM/IEEE Symposium on Logic in Computer Science*, pp. 573–584. doi:10.1109/LICS.2015.59.
- [8] Amar Hadzihasanovic (2017): *The algebra of entanglement and the geometry of composition*. Ph.D. thesis, University of Oxford. arXiv:1709.08086.
- [9] Amar Hadzihasanovic, Kang Feng Ng & Quanlong Wang (2018): *Two Complete Axiomatisations of Pure-state Qubit Quantum Computing*. In: *Proceedings of the 33rd Annual ACM/IEEE Symposium on Logic in Computer Science*, LICS ’18, ACM, pp. 502–511. doi:10.1145/3209108.3209128.
- [10] Emmanuel Jeandel, Simon Perdrix & Renaud Vilmart (2018): *Diagrammatic Reasoning Beyond Clifford+T Quantum Mechanics*. In: *Proceedings of the 33rd Annual ACM/IEEE Symposium on Logic in Computer Science*, LICS ’18, ACM,

New York, NY, USA, pp. 569–578, doi:10.1145/3209108.3209139. Available at <http://doi.acm.org/10.1145/3209108.3209139>.

- [11] Saunders MacLane (1965): *Categorical algebra*. *Bulletin of the American Mathematical Society* 71(1), pp. 40–106. <https://projecteuclid.org:443/euclid.bams/1183526392>.
- [12] Kang Feng Ng & Quanlong Wang (2018): *Completeness of the ZX-calculus for Pure Qubit Clifford+T Quantum Mechanics*. arXiv:1801.07993.
- [13] Quanlong Wang (2020): *An algebraic axiomatisation of ZX-calculus*. *Proceedings of the 17th International Conference on Quantum Physics and Logic (QPL) 2020*. ArXiv:1911.06752.
- [14] Quanlong Wang (2020): *Algebraic complete axiomatisation of ZX-calculus with a norm form via elementary matrix operations*. ArXiv:2007.13739.
- [15] Quanlong Wang (2020): *Enter a visual era: process theory embodied in ZX-calculus*. Presentation at 17th International Conference on Quantum Physics and Logic (QPL), doi:10.13140/RG.2.2.17289.67682.